POLITECNICO DI MILANO

School of Information and Industrial Engineering

Electronic, Information and Bioengineering Department

Master of Science in

Telecommunications Engineering

Space and time evolution of synthetic rain structures

Supervisor: Prof. Carlo Capsoni

Graduation thesis of:
Simone Ghirardin
ID: 805529

Academic year 2015-2016

Author: *Simone Ghirardin*

Ringraziamenti

Ringrazio innanzitutto il mio relatore, il professor Carlo Capsoni, per avermi proposto questa tesi, per tutti i consigli e per l'immensa pazienza che ha avuto nell'aiutarmi. Ringrazio inoltre Lorenzo Luini per i suoi preziosi suggerimenti e per il materiale che mi ha fornito, utile per completare il mio lavoro.
Un ringraziamento particolare va a mia mamma e a mio papà che mi hanno sempre sostenuto durante tutto il percorso di studi, certi che ce l'avrei fatta.
Infine vorrei ringraziare i miei compagni più stretti Eva, Mizi, Gioele, i tesisti e i dottorandi con cui ho passato quest'ultimo periodo e tutti gli altri miei amici più cari per aver sempre creduto in me.

Abstract

The thesis aims at developing an application that emulates an environment affected by rainfall in order to evaluate the possible effects that the radio channel may be subject.
Throughout the work, will be crucial the model EXCELL, studied at the Politecnico di Milano, which reproduces the statistical characteristics of a real rain cell.
In the first part of the thesis the application will focus on the modeling of a single rainy cell with time variable characteristics, that interferes with a radio link established between two devices. The cell will have the possibility to move within the environment, in order to characterize a scene as more realistic as possible (using physical parameters such as wind direction and speed) and it will interfere with the radio channel by introducing a certain attenuation. The signal transmitted at a frequency between 20 and 70 GHz is strongly affected by the attenuation due to the characteristics of the rain passing over the radio channel, in particular by its rainy intensity, measured in mm/h, by its area and by the length of the radio link involved. Our task will be to study the behavior of the attenuation as a function of the parameters for the link and the cell used.
In the second part of the thesis we will proceed to give a representation of the amount of water and its percentage changes within a radar map, composed of different rainy masses called aggregates, with their own dynamics and dependent on the evolution of the amount of water present in the map.
The aggregates, in turn, are defined by a number of cells whose behavior needs to be properly implemented. The latter will be synthesized with the model EXCELL and it will follow the physical characteristics observed in reality. In particular, they will have the opportunity to evolve according to their nature or to dissolve according to the fulfillment or otherwise of certain conditions.

Sommario

La tesi si propone di sviluppare un' applicazione in grado di emulare un ambiente affetto da precipitazioni in modo da poter valutare i possibili effetti a cui il canale radio potrebbe essere soggetto.
In tutto il lavoro, di fondamentale importanza sarà il modello EXCELL, realizzato al Politecnico di Milano, che riproduce le caratteristiche statistiche di un cella di pioggia reale.
Nella prima parte della tesi l'applicazione verterà sulla modellizzazione di una singola cella piovosa con caratteristiche tempo variabili che interferisce con un link radio instaurato tra due apparati. La cella avrà la possibilità di muoversi all'interno dell'ambiente, in modo da caratterizzare una scena più realistica possibile (utilizzando parametri fisici quali direzione e spostamento del vento) e interferirà con il canale radio introducendo una certa attenuazione. Il segnale trasmesso alla frequenza tra i 20 e 70 GHz è affetto fortemente dall'attenuazione dovuta alle caratteristiche della pioggia che lo attraversa, in particolare dalla sua intensità piovosa, misurata in mm/h, dalla sua area e dalla lunghezza del link radio interessata. Sarà quindi nostro compito studiare il comportamento dell'attenuazione in funzione dei parametri per il link e per la cella utilizzati.
Nella seconda parte della tesi ci si preoccuperà di dare una rappresentazione della quantità d'acqua e delle sue variazioni percentuali all'interno di una mappa radar, costituita da diverse masse piovose, chiamate aggregati, con una propria dinamica e dipendenti dall'evoluzione della quantità d'acqua presente nella mappa.
Gli aggregati a loro volta sono definiti da un certo numero di celle il cui comportamento deve essere correttamente implementato. Quest'ultime saranno sintetizzate con il modello EXCELL e seguiranno le caratteristiche fisiche osservate nella realtà. In particolare, avranno la possibilità di evolvere in funzione della loro natura o di dissolversi in base allo soddisfacimento o meno di determinate condizioni.

Contents

List of Figures

List of Tables

Introduction

The evolution of telecommunication systems, both terrestrial and earth to satellite and the continuous electronic technologic development, is always pushing towards the use of higher transmission frequencies (Ka, 27-40 GHz, and Q/V bands, 50-75 GHz), mainly due to the congestion of lower frequency bands (Ku, 12-18 Ghz) and to the always increasing demand of bandwidth for real-time multimedia services that require reliability and the desired system availability for the end user.
Telecommunication links operating at this high frequencies, mainly above 10GHz, are strongly affected by attenuation, polarization and scattering phenomena caused by atmospheric impairments like rain, that plays the prevailing role, hail, ice crystals, or wet snow [2].
Moreover, in this environment, strong signal fades can no longer be overcome by making use of static power margins, but require the application of Fade Mitigation Techniques (FMTs), such as time diversity and site diversity, to offer a sufficient quality of service to the user point of view [3].
As an alternative to FMTs, rain fields collected by weather radars represent the most suitable source of information, as simulations based on such kind of data inherently reflect the influence of the local climatology and topography .
However, the lack of worldwide comprehensive and reliable precipitation data has pushed towards the development of models to represent at best the characteristics of the local rainfall process, both in terms of first-order (e.g. probability density function) and of second-order (e.g. temporal correlation and spatial distribution) statistics. Among the various approaches to rain field modeling proposed in the literature so far (meteorological, statistical, stochastic, fractal models), those relying on the cellular representation are particularly suitable for applications related to the radio propagation through the atmosphere [4].
In Chapter 1 it will be presented the description of the cellular models most utilized, their properties and their morphological characteristics. In particular, it will be given in detail a description of the EXCELL [5], studied in Politecnico di Milano, and the HYCELL [6] followed by a brief description of SC-EXCELL [7].
In the Chapter 2 it will be presented the simulator relative to a synthetic cell that evolves during its movement and passes through a radio channel introducing a certain level of attenuation that will be analyzed.

Finally, in the chapter 3 it will be extended the concept of single cell to an aggregate of more cells. After the description of the evolution of the water quantity of the aggregate inside the map, it follows the description of the behavior of the cells, modeled with EXCELL, pertaining to a specific aggregate. Furthermore, it will be studied other aspects regarding the reciprocal behaviors among the cells and their elimination at the end of their life.

Chapter 1

Theoretical cellular models

1.1 Rain cell models

A rain cell is defined as a region of space composed of connected points where the rain rate exceeds a chosen threshold.
A model, in this case synthetic cell, can be used to represent a radar cell on the basis of meteorological data: in both cases the action exerted by rain patterns on the radio system (single or multiple links) can be studied by simulating the relative motion of the patterns with respect to the radio system and evaluating, in any position, the parameter of interest (attenuation, interference,etc.), which can, at the end of the process, be described statistically [5]. Moreover, the model cell, only defined by a few parameters, has the significant advantages of less computing time and storage, and offers the possibility of transforming the statistics of rain cells obtained at a given site to a new set of statistics relevant to user's site on the basis of local pluviometric data.
Two well known rain cell models include the EXCELL model [6] and the HYCELL model [7].

1.2 EXCELL Model

The observation of 6215 cells collected by the 3D meteorological radar in Spino d'Adda, near Milan, in 1980 from April to October, comprising almost the totality of the rain events of the year, were used to investigate the spatial distribution of the cells. The radar data collected were processed to generate reflectivity maps

on a horizontal plane at approximately 1.5 kilometers above the ground level. The resulting images were remapped to a Cartesian grid with a resolution of 1x1 km^2 and after converting the reflectivity Z into the rain rate R [mm/h] through the Marshall-Palmer relationship. Rain cells were identified as areas encircled by 5 mm/h contour.

The study of the radar cells points out a set of descriptors of integral nature:

Cell area

$$A = \int_{CELL} dxdy \tag{1.1}$$

Cumulative rain

$$Q = \int_{CELL} R(x,y)dxdy \tag{1.2}$$

Average rain rate

$$\overline{R} = Q/A \tag{1.3}$$

Root mean square rain rate

$$R^2_{rms} = \frac{1}{A}\int_{CELL} R^2(x,y)dxdy \tag{1.4}$$

To account for the spatial asymmetry of cells the following "geometrical" descriptors are evaluated:
Cell barycenter, the point of coordinates

$$x_0 = \frac{1}{Q}\int_{CELL} xR(x,y)dxdy \tag{1.5}$$

$$y_0 = \frac{1}{Q}\int_{CELL} yR(x,y)dxdy \tag{1.6}$$

Central moment of inertia

$$I_x = \int_{CELL} (x - x_0)^2 R(x, y) dxdy \tag{1.7}$$

$$I_y = \int_{CELL} (y - y_0)^2 R(x, y) dxdy \tag{1.8}$$

Considering I_{min} and I_{max} respectively the minimum and maximum between I_x and I_y we can calculate the "gyration radii" of the cell

$$\rho_{max}^2 Q = I_{max} \tag{1.9}$$

$$\rho_{min}^2 Q = I_{min} \tag{1.10}$$

which allow us to define the cell ellipticity as

$$\rho_{min}/\rho_{max} \tag{1.11}$$

The evaluation of these parameters has been used to define an analytic model that optimally reproduce the point rain rate cumulative distribution, P(R), produced by the whole population of measured cells. It turned out that the rain intensity distribution within a single cell is usually characterized by a peak value, and that, moving away from it, the rain rate steeply decreases. This behavior is well approximated by an exponential model that can be described, assuming a reference system along the principal axes, by the functions

$$R = R_M exp\left[-\sqrt{\left(\frac{x^2}{\rho_x^2} + \frac{y^2}{\rho_y^2} \right)} \right] \tag{1.12}$$

in the bi-axial model, and

$$R = R_M exp\left[-\frac{\sqrt{(x^2 + y^2)}}{\rho_0} \right] \tag{1.13}$$

in the mono-axial model.

In (1.12) and in (1.13) R_M is the peak rain rate, ρ_x, ρ_y and ρ_0 are the distances (cell radii) along the respective axes for which rain rate decreases by a factor $1/e$. Every cell is obtained forcing cells descriptors to be the same in the radar and in the model and choosing the one which best complied with the fundamental prerequisite concerning P(R). In particular, the fitting is applied on the cell area A and on the average rain rate $\overline{R}$ (1.1),(1.3 of radar cell to the A and $\overline{R}$ of the model cell, given by the expressions

$$A = \pi \rho_x \rho_y ln^2(R_M/R_{th}) \tag{1.14}$$

with rain rate threshold $R_{th} = 5mm/h$ and in particular for the mono-axial model with $\rho_0 = \rho_x = \rho_y$

$$A = \pi \rho_0^2 ln^2(R_M/R_{th}) \tag{1.15}$$

and

$$\overline{R} = 2R_M[1 - (R_{th}/R_M)(1 + ln(R_M/R_{th}))]/ln^2(R_M/Rth) \tag{1.16}$$

with $R_{th} = 5mm/h$ and $R_M \geq 5mm/h$.
The expression giving the cell ellipticity is

$$\rho_x/\rho_y = \rho_{min}/\rho_{max} \tag{1.17}$$

which completes the set of the fit-forcing equations for the biaxial model.

Other two tests had been made on R_{rms} and R_M to evaluate the quality of the model:

- The analysis R_{rms} gived by the formula

$$R_{rms} = R_M \sqrt{\frac{1 - (R_{th}/R_M)(1 + 2ln(R_M/R_{th}))}{2ln^2(R_M/Rth)}} \tag{1.18}$$

  showed that in most cases it can be predicted from $\overline{R}$ using an exponential model with an error less than $10mm/h$ and that only a small number of cells contributes to major deviation (probability level of 10^{-3}).

- The model cells show an overestimation of the measured R_M that compensate the underestimation of radar measured peak values, affected by the spatial filtering in the 1 x 1 km^2 grid element.

- The cell asymmetry ρ_x/ρ_y, whose average value is about 0.56, has be found to be uncorrelated to the cell size and the peak intensity.

These results points out that long-term statistics of point rain rate for a given site associated with the number of occurrence $N(R_M, \rho 0)$ (proportional to the probability of occurrence for a synthetic cell with peak rain rate of R_M and a certain $\rho 0$) in all locations, make possible the extension of the empirical results obtained in a test site to any other site for general prediction purposes. Thanks to its simplicity, EXCELL results to be the most adequate to be represented. Moreover, it is demonstrated that the rain cells within the rain maps collected by the meteorological radar don't have preferential direction of rotation. This peculiarity points out that is possible to use a mono-axial EXCELL model instead of a bi-axial EXCELL model and for this reason in the entire work it will be considered the mono-axial one.

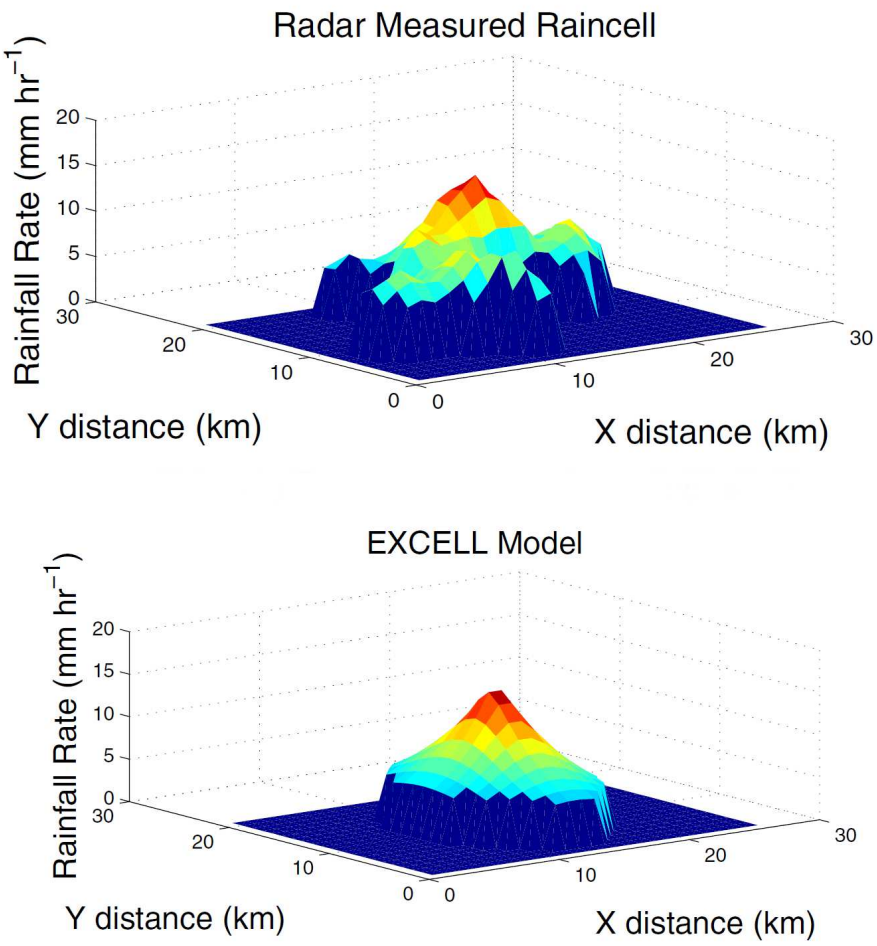

Figure 1.1: Difference between radar cell and corresponding synthetic exponential cell.

1.3 HYCELL Model

The HYCELL model was developed on the basis of CAPPI (Constant Altitude Plane Position Indicator) radar images collected by the observation of thousands

of cells in the regions of Bordeaux (southwestern France) and Karlsruhe (southwestern Germany). The two sites are at midlatitude but the climatic contexts differ: oceanic for Bordeaux and continental for Karlsruhe.
Studying the structure of the radar cells it was noticed that usually, convective cells are surrounded by a stratifom area where the rain rate is weaker. This feature can't be described with an exponential function, for three meaningful reasons:

- it doesn't account for the differences between convective and stratiform type of rain: is not always suited for the description of the rain rate horizontal distribution in the convective part of the cell.
- isolated punctual maxima of rain rate are not usually observed in nature. In fact, radar observations show that, at all latitudes, the rain rate horizontal distribution in the vicinity of the rain cell peak does not decay as abruptly as what an exponential function would describe but rather as what a Gaussian one would.
- it doesn't optimally reproduce the rain rate distribution in the case of rain cells which exhibit high rain rates on non negligible areas (for example rain cells constituting tropical rains, monsoon rains or even summer storms in mean latitudes). In these cases, the fit forcing equation on the average rain rate leads to overestimate the peak rain rate of the cell.

To overcome these limitations, a possibility is to consider a hybrid modeling, where the horizontal rainfall rate distribution is described with a combination of an exponential shape, that accounts for the stratiform part of the cell, and the Gaussian shape that accounts for the convective one.

The analytical expression for the *HYCELL* model is:

$$R = R_G exp\left[-\left(\frac{x^2}{a_G^2} + \frac{y^2}{b_G^2}\right)\right] \quad if\ R \geq R_1 \tag{1.19}$$

$$= R_E exp\left[-\left(\frac{x^2}{a_E^2} + \frac{y^2}{b_E^2}\right)\right] \quad if\ R_2 \leq R < R_1 \tag{1.20}$$

where R_G is peak rainfall rate of the Gaussian component, a_G and b_G are distances along x and y axes where the rainfall rate decreases by a factor of $1/e$ of the Gaussian component. R_E, a_E and b_E are defined the same for the exponential component. R_1 is the rainfall rate that separates the Gaussian and exponential components.

The HYCELL model uses a set of force fitting equations that are solved to determine the seven parameters of the model. The HYCELL model also requires the horizontal gradient of the measured cell, where the mean, $\overline{G}$, and root mean squared (RMS), G_{rms} are taken.

The mean gradient is given by

$$\overline{G} = \frac{1}{A}\int_{CELL} G(x,y)dxdy \tag{1.21}$$

where G(x, y) is the horizontal gradient at coordinates x and y. The root mean squared gradient is given by

$$\overline{G}^2_{rms} = \frac{1}{A}\int_{CELL} G^2(x,y)dxdy \tag{1.22}$$

The radar measured cell must be rotated for the horizontal gradient to be calculated. The angle of rotation is given by the following

$$\theta = \frac{1}{2}tan^{-1}\left(\frac{2I_{xy}}{I_y - I_x}\right) \tag{1.23}$$

where I_{xy} is the moment of inertia in the barycenter reference, as defined below

$$I_{xy} = \int_{CELL}(x-x_0)(y-y_0)R(x,y)dxdy \tag{1.24}$$

The following equations give the HYCELL model average rainfall rate, root mean square rainfall rate, average horizontal gradient and root mean squared gradient]. Parameter R_G, R_1 and R_E may be determined by solving equations (1.25)-(1.28)

$$\begin{aligned}\overline{R} = ln^{-2}\left(\frac{R_E}{R_2}\right)\Big[ln^2\left(\frac{R_E}{R_1}\right)ln^{-1}\left(\frac{R_G}{R_1}\right)(R_G - R_1)\\ 2R_1\left(1+ln\left(\frac{R_E}{R_1}\right)\right) - 2R_2\left(1+ln\left(\frac{R_E}{R_2}\right)\right)\Big]\end{aligned} \tag{1.25}$$

$$2(R_{rms}^2) = ln^{-2}\left(\frac{R_E}{R_2}\right)\left[ln^{-1}\left(\frac{R_G}{R_1}\right)ln^2\left(\frac{R_E}{R_1}\right)(R_G^2 - R_1^2) + R_1^2\left(1 + 2ln\left(\frac{R_E}{R_2}\right)\right) - R_2^2\left(1 + 2ln\left(\frac{R_E}{R_2}\right)\right)\right] \tag{1.26}$$

$$\overline{G} = \frac{4E\left[\frac{\pi}{2}, (1-e_r^2)^{1/2}\right]}{(A\pi e_r)^{1/2} ln\frac{R_E}{R_2}}\left[R_G\frac{\pi^{1/2}}{2}erf\left(ln^{1/2}\frac{R_G}{R_1}\right)ln\left(\frac{R_E}{R_1}\right) \cdot ln^{-1/2}\frac{R_G}{R_1} + R_1 - R_2\left(1 + ln\frac{R_E}{R_2}\right)\right] \tag{1.27}$$

$$A(G_{rms}^2) = \frac{\pi}{2}\left(e_r + \frac{1}{e_r}\right)\left[R_G^2 - R_1\left(1 + 2ln\frac{R_G}{R_1}\right) + \frac{R_1^2}{2}\left(1 + 2ln\frac{R_E}{R_1}\right) - \frac{R_2^2}{2}\left(1 + 2ln\frac{R_E}{R_2}\right)\right] \tag{1.28}$$

To solve the set of equations (1.25)-(1.28), a minimization function (1.29) was used. The subscripts represent the difference between radar measured data (i.e. radar measured average rainfall rate R_r) and HYCELL model (i.e. HYCELL average rainfall rate R_H).

$$\epsilon = \left|\frac{\overline{R_H}}{\overline{R_r}} - 1\right| + \left|\frac{(R_{rms})_H}{(R_{rms})_r} - 1\right| + \left[\frac{\overline{G_H}}{\overline{G_r}} - 1\right] + \left|\frac{(G_{rms})_H}{(G_{rms})_r} - 1\right| \tag{1.29}$$

Once R_G, R_1 and R_E have been determined by minimizing (1.29), the remaining four parameters, a_G, b_G, a_E and b_E are solved by substituting calculated values into the following;

$$b_E^2 = \frac{A_r}{\pi e_r ln^2\frac{R_E}{R_2}}, a_E = e_r b_E \tag{1.30}$$

$$b_G^2 = \frac{b_E^2 ln^2\frac{R_E}{R_1}}{ln\frac{R_G}{R_1}}, a_G = e_r b_G \tag{1.31}$$

In Fig. 1.2 is possible to observe a comparison between the horizontal profile of EXCELL and the horizontal profile of HYCELL, with the parameters just above described. It should also be noted that the peak of the rain cell generated by means of EXCELL presents a peak lower than that one generated by means

of HYCELL. The HYCELL and the EXCELL shows the same slope until R_1, after this value the former evolves following a Gaussian function, while the latter following the exponential function.

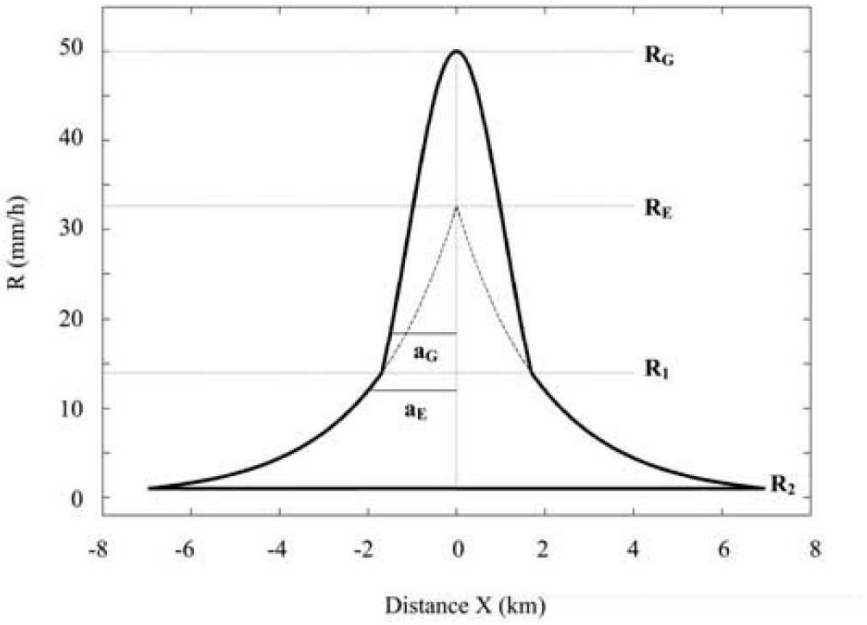

Figure 1.2: Comparison between EXCELL and HYCELL horizontal profiles.

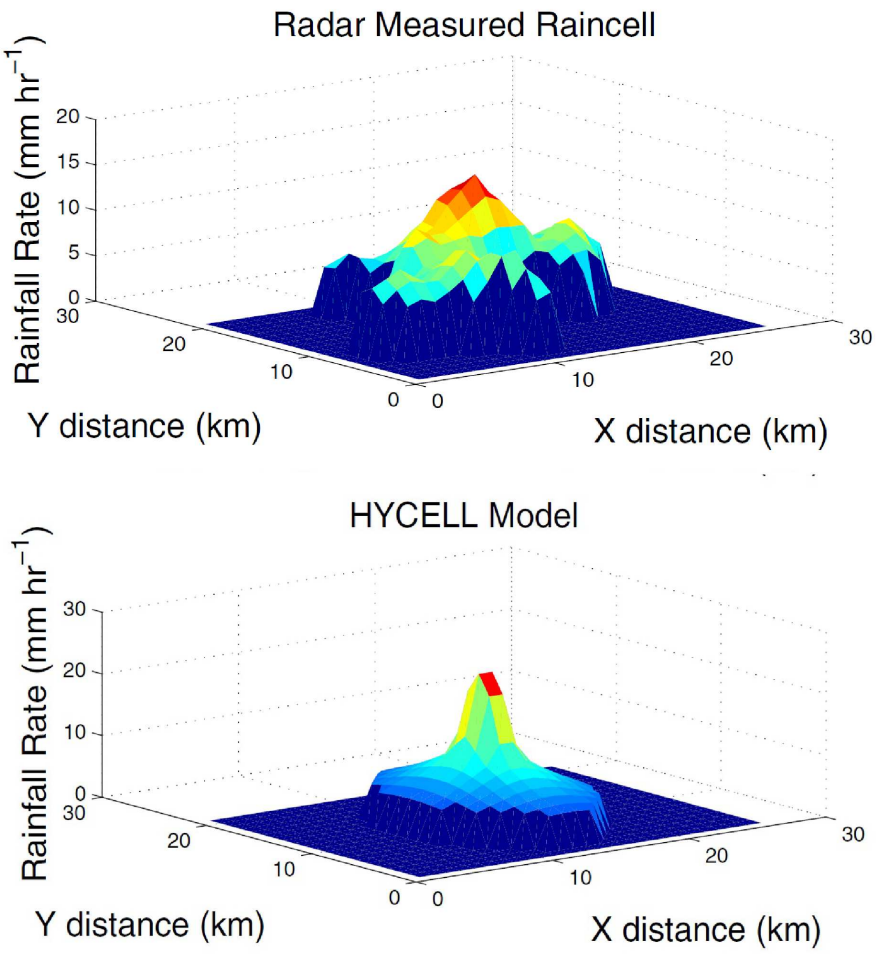

Figure 1.3: Difference between radar cell and corresponding synthetic hybrid cell.

It is worth mentioning that the hybrid Gaussian-exponential cell profile defined in the HYCELL model certainly provides a slightly more accurate representation of real rain cells, but at the expenses of a much more complicated modeling: in fact, the identification of Gaussian-exponential cells require seven parameters, instead of two, and the relationship between the cells' number density and the local P(R), which is the quantity necessary to implement the model, is quite cumbersome [3].

1.4 Other Models

In this chapter are presented an enhanced version of EXcell model, the SC EXCELL and are briefly referenced other non cellular models.

1.4.1 SC EXCELL

This model was developed to use it in different climatic regions characterized by rain rate with different intensities. In particular, as many authors proposed in literature, the rain cell population can be divided into two groups:

- *stratifom cells* characterized by a slow decay of the rain rate from its maximum (which is usually chosen less than $10mm/h$). They can extend to several hundreds of kilometers horizontally, and can be reasonably assumed to extend up to the 0Â°C isotherm height, vertically (four to six kilometers).
- *convective cells*, representing an area of heavy rain with intensities higher than $10mm/h$. They are often associated with thunderstorm events, are of much smaller horizontal extent with respect to stratiform cells, usually only several kilometers, but can extend to much greater vertical heights, due to the presence of strong updrafts and downdrafts, which also prevent the formation of the melting layer (that is associated with stratiform rainfall). They are typical of equatorial and tropical regions.

The SC EXCELL version improves the EXCELL by introducing the capability to discriminate between stratiform and convective rain cells [7]. Rain fields are represented by exponentially shaped rain cells, for which the rain intensity is defined as:

$$R(\rho) = (R_M + R_{low})e^{-\frac{\rho}{\rho_0}} - R_{low} \quad (mm/h) \tag{1.32}$$

where ρ is the distance from the cell center, where the peak R_M is located, ρ_0 is the equivalent radius for which the rain intensity is equal to R_M/e, and R_{low} is the lowering factor allowing the rain profile $R(\rho)$ to reach zero at finite distance from the cell center. The probability of rain cells occurrence is derived from the 1-min integrated P(R) of the site and is dependent on R_M and ρ_0. The physical structure of the SC EXCELL model allows to discriminate, on a statistical basis, between stratiform and convective cells, so that the yearly P(R) results in a combination of the P(R)s relative to each type of precipitation. The discrimination is based on the yearly $P(R)$ and leads to define a threshold peak value $R_{M,th}$, for which

cells characterized by $R_M < R_{M,th}$ contribute to $P(R)_{str}$, the remaining ones to $P(R)_{cnv}$. As a matter of fact, $R_{M,th}$ ranges from 14 to 17 mm/h depending on the input $P(R)$.
Furthermore, the model take into account the rain height for the two groups that play an important role in determining the effective path length that suffers from rain attenuation. In particular as derived from ERA-15 meteorological database,

$$h_{str} = \frac{\sum_{i=1}^{12} \alpha_i p_i h_i}{\sum_{i=1}^{12} \alpha_i p_i} \qquad h_{cnv} = \frac{\sum_{i=1}^{12} \beta_i p_i h_i}{\sum_{i=1}^{12} \beta_i p_i} \tag{1.33}$$

where h_i is monthly mean values of the 0°C isotherm height, β_i is the monthly convective rain amount over the total rain amount, p_i monthly probability of rainy period for 6-hour , $\alpha_i = 1 - \beta_i$ and finally $i = 1...12$ is the index of the month. Stratiform events are usually characterized by the presence of the melting layer which cause extra attenuation. The contribution of the bright band to attenuation can be taken into account by introducing the equivalent rain layer height H_{BB} can be expressed as a function of the frequency f through the equation below:

$$H_{BB} = 4.5788e^{-0.0675f} + 0.51 \ (km) \tag{1.34}$$

To calculate the effective stratiform rain height, the equivalent bright band rain height needs to be added to the stratiform rain height:

$$H_{strRain} = h_{str} + H_{BB}(f) \ (km) \tag{1.35}$$

In the convective events, rain height most likely exceeds the 0°C isotherm height; the SC EXCELL model takes into account this behavior by increasing by 20% the value of h_{cnv}. Consequently, the effective convective rain height assumes the following expression:

$$H_{cnvRain} = 1.2h_{cnv} \ (km) \tag{1.36}$$

1.4.2 Non cellular models

Non cellular models is developed with the aim to describe at best spatial structure and temporal evolution. The best known are *meteorological* (physical model), *stochastic*, *fractal* and *statistical*. Compared to the cellular models they are not particularly suited for the analysis of the issues related to the radio propagation through the atmosphere.

Chapter 2

Attenuation of a moving EXCELL

In this chapter it is presented the implementation of a scenario where a single cell moves along a fixed path. After the description of scenario parameters (dimension of map, length of the radio link, time resolution) and the cell parameters (velocity and direction of the cell, height of the cell) set by the user and the comparison of the attenuation contribution in the case of static cell and dynamic cell, it follows the specification of the spatial and temporal evolution theory used in this scheme.

2.1 Scene parameters

2.1.1 Map dimension

The dimensions of the map have been chosen taking into account previous works effectuated on databases derived by the Spino d'Adda radar, the NPC and the LR database [8]. Both are constituted of pseudo CAPPI snapshots: the former has spatial resolutions and operational range of 0.5 x 0.5 km and 150 km, the latter has spatial resolutions and operational range of 0.5 x 0.5 km^2 and 40 km resulting in a grid of 160 x 160 pixels (80 x 80 km^2).
These databases are composed by 3D or 2D grids of pixels (rain rate values) containing reflectivity levels that were remapped to the corresponding rain rate values by means of the Marshall-Palmer Law:

$$Z = 200R^{1.6} \tag{2.1}$$

With this consideration in mind, to maintain the matching between radar maps

and the synthetic one, built by means of EXCELL model, it is useful to utilize the same typology of matrix: the matrix represents a field with a square base containing the rain rate values of the chosen synthetic exponential cell.
The dimensions of the pixels represents the resolution of the map that must be chosen based on what is the necessary level of precision to best represent the exponential cell and its movement.
It is worth observing that a high resolution is not always necessary because, although higher resolutions are useful to describe better the synthetic cell within the matrix and to commit a relative lower error in the calculation of the attenuation with respect to a matrix chosen with a lower resolution, it could lead to have big matrix computationally hard to handle; this issue can be quite cumbersome when the study is applied on thousands of matrix with these dimensions containing more than one cell.
It is noticed that the best results are obtained by utilizing a map with resolution of the pixel of 100 x 100 m^2.

2.1.2 Radio link parameters

In this work, the application can refer to a link positioned on the ground or to a typical configuration Earth-space link where transmitter and the receiver (a geosynchronous satellite), are fixed during the scene and are positioned in coordinates defined by the user.
Given the position of transmitter P_{tx} and the position of receiver P_{rx} defined in a 3D space that describes the field analyzed, the distance between the two stations is

$$L_E = |P_{tx} - P_{rx}| = \sqrt{(x_{tx} - x_{rx})^2 + (y_{tx} - y_{rx})^2 + (z_{tx} - z_{rx})^2} \quad [m] \qquad (2.2)$$

the elevation angle is calculated with the expression

$$\theta = \tan^{-1}\left(\frac{|z_{tx} - z_{rx}|}{\sqrt{(x_{tx} - x_{rx})^2 + (y_{tx} - y_{rx})^2}}\right) \quad [rad] \qquad (2.3)$$

The operative frequencies must be chosen possibly taking into account the values where the link is affected by rain, in particular the frequency between 10 and 60 GHz. These parameters with the wave polarization(always defined by the user), are fundamental in the calculation of the attenuation of the link affected by rain; in particular they are used, with reference to the recommendation of ITU-R 838-1

to calculate the specific attenuation defined by the expression:

$$\gamma_R = kR^{\alpha} \tag{2.4}$$

with α and k rain rate-to-specific attenuation conversion coefficients that depend on the hydrometeors properties (e.g. Drop Size Distribution, DSD, and temperature), on the link elevation angle, on the wave polarization, and, mainly, on the operational frequency [9]. They are given in Table 2.1 for linear polarizations (horizontal: H, vertical: V) and horizontal paths for frequencies most used in terrestrial and satellite communication.

$$k = \left[k_H + k_V + (k_H - k_V)\cos^2\theta\cos 2\tau\right]/2 \tag{2.5}$$

$$\alpha = \left[k_H\alpha_H + k_V\alpha_V + (k_H\alpha_H - k_V\alpha_V)\cos^2\theta\cos 2\tau\right]/2k \tag{2.6}$$

where θ is the path elevation angle and τ is the polarization tilt angle relative to the horizontal ($\tau = 45°$ for circular polarization).

Table 2.1: Regression coefficients for estimating specific attenuation.

Frequency (Ghz)	k_H	k_V	α_H	α_V
12	0.0188	0.0168	1.217	1.200
15	0.0367	0.0335	1.154	1.128
20	0.0751	0.0691	1.099	1.065
25	0.124	0.113	1.061	1.030
30	0.187	0.167	1.021	1.000
35	0.263	0.233	0.979	0.963
40	0.350	0.310	0.939	0.929
45	0.442	0.393	0.903	0.897
50	0.536	0.479	0.873	0.868
60	0.707	0.642	0.826	0.824
70	0.851	0.784	0.793	0.793

2.1.3 Time resolution

The duration of the scene T [s] is related to the movement of the cell and is defined by the necessary time to allow the cell to pass through the link. The time T_s [s], instead, is defined by the user and describes how often occurs the scanning of the parameters and therefore the calculation of the attenuation. It is important to underline that this period must be chosen being careful on the velocity of the cell and the resolution of the matrix: if the period is in the order of few seconds and the speed of the cell is low, with a low resolution it would not observe variations for the attenuation that would remain the same because the cell would not go through the pixel completely.

2.2 Physical cell parameters

2.2.1 Wind speed an direction

The speed and direction of the wind are fundamental parameters to define the displacement of the cell. In a previous work on two radar datasets [8] collected in two temperate sites, Spino d'Adda, Italy $(45.4°N, 9.5°E)$ and Bordeaux $(44.5°N, -0.34°E)$ has been analized different levels of pressure: 850, 775, 700, 600, 500 hPa, corresponding roughly to heights between 1.5 and 5.5 km. The wind direction, as illustrated in Fig. 2.1, is related on the characteristics of the territory: in Bordeaux, that lies in the proximity of the ocean and whose area is not characterized by a significant orography, is mainly eastward while in Spino d'Adda, air fluxes from the North are blocked by the Alps and consequently, most of the time, air streams flow from West or South.

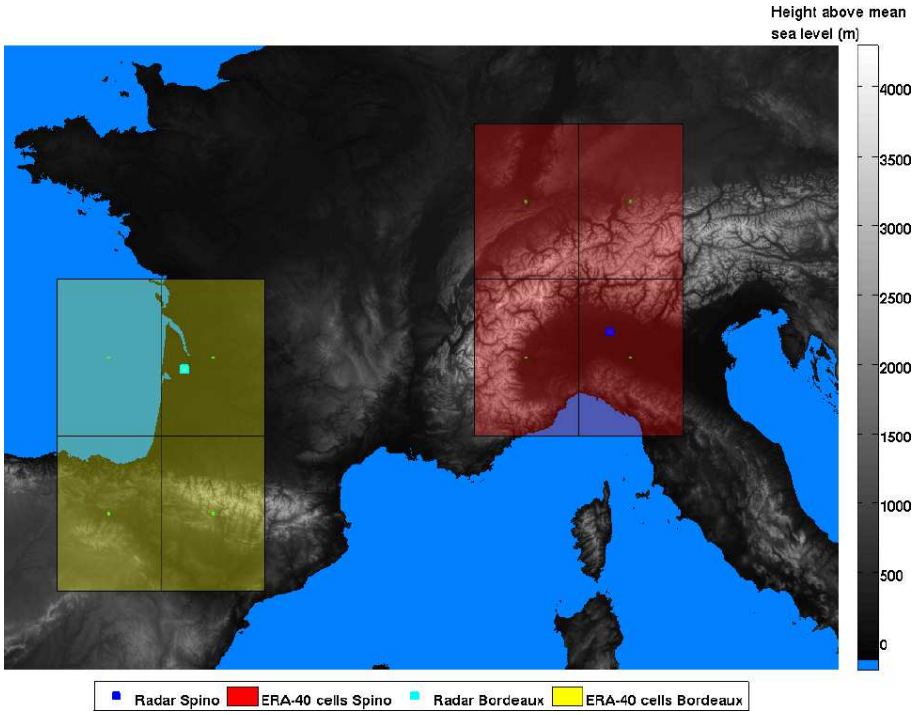

Figure 2.1: Position of the observation area and of the cells of the reanalysis model.

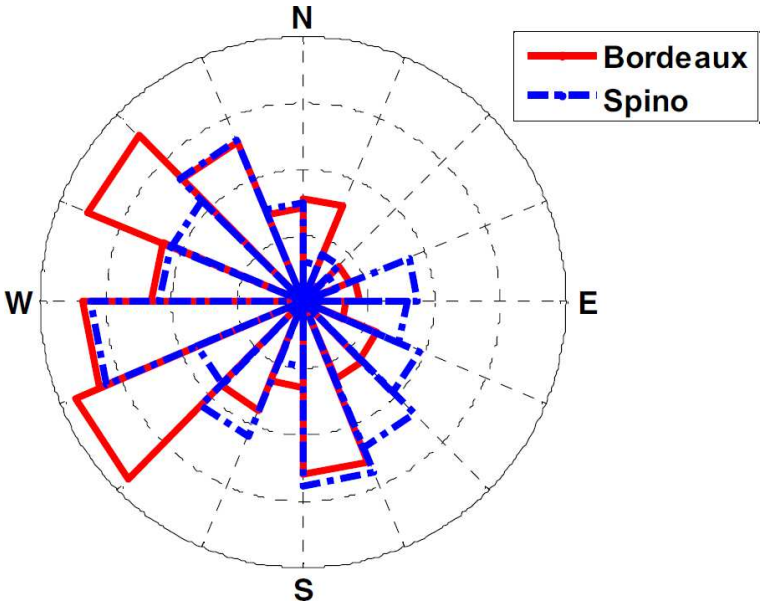

Figure 2.2: Distribution of the wind direction at 775hPa computed from one year of ERA-40 data for Spino d'Adda and Bordeaux.

The study showed that the correlation between the rain advection derived from radar datasets and from the ECMWF (European Center for Medium-range Weather Forecast) ERA-40 meteorological database, wind data at several pressure levels presents the highest overall correlation at the 700 hPa isobar as listed in the table below.
Lower levels (850 hPa, 775 hPa) underestimate the rain advection speed, as well as higher layers tend to overestimate it. Moreover, the direction estimation is perturbed at lowest levels by the proximity to the ground.
With this consideration in mind, the parameters must be realistic for the area where is set the scene: for example, for an ambient with pressure of 700 hPa, plausible values to choose for the wind speed can be between 10 and 60 km/h (in Spino d'Adda as shown in Fig. 2.3) with and an advection towards west.

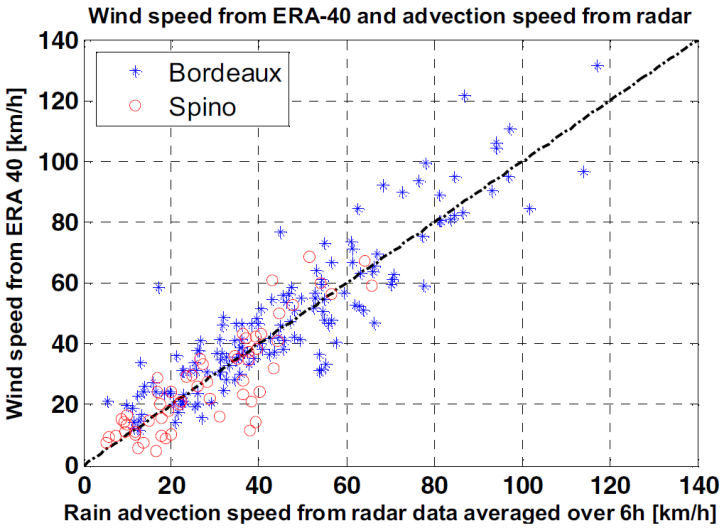

Figure 2.3: ERA-40 wind speed at 700 hPa versus rain advection speed for Bordeaux and Spino d'Adda.

In the simulator the user can choose the direction of the cell setting its initial and final position described by two couples $(x_0, y_0), (x_f, y_f)$ and the uniform speed to which the cell moves, V [m/s].
These parameters are used to generate two arrays with length T representing the evolution of x and y coordinates during the scene. In particular, every element of the arrays will be:

$$\boldsymbol{x}(n) = x_0 + nV cos(\phi)$$
$$\boldsymbol{y}(n) = y_0 + nV sin(\phi)$$

with n=1,2...T and ϕ represents the angle between initial and final position of the cell on the x-y plane by the expression

$\phi = tan^{-1}\left(\frac{y_f - y_0}{x_f - x_0}\right)$

The elements are rounded at the nearest integer so that they can be used as indexes of rows (displacement along x axis) and columns(displacement along y axis) within the matrix. The position of the cell during the scene will be updated based on this indexes.

2.2.2 Cloud Height

The cloud height defines the position where the rain doesn't affect anymore the radio link. In this work, it is possible to use the recommendation ITU-R 839.4 [10] utilized for areas of the world where no specific information is available, the expression of the mean annual rain height above mean sea level is:

$$H = h_0 + 0.36km \tag{2.7}$$

where h_0 is the mean annual 0° C isotherm height above mean sea level (an integral part of the Recommendation) and is available in the form of a digital map provided in the file available on the site `http://www.itu.int/rec/R-REC-P.839-4-201309-I/en`.
In this work the height of the cell is maintained fixed during the simulation, although this should not be actually true: as explained previously in the chapter of the SC EXCELL the height also depends on the characteristics of the rainfall, where convective rains shows higher heights with respects stratiform rains.

The scheme below give a simple description of the environment with a radio channel between a base station and a satellite far L_E [km] and affected by a rain cell.

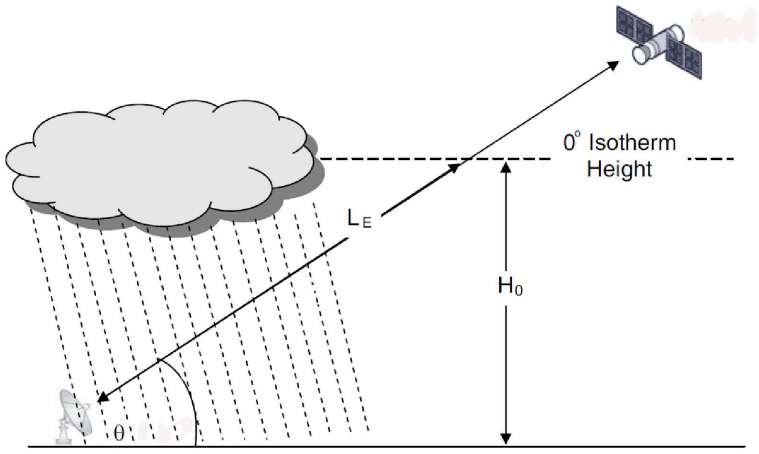

Figure 2.4: Schematic diagram of earth-space communication affected by rain [1].

2.3 Horizontal profile evolution

As suggested in Chapter 1 the following exponential expression has been used in this work as analytic model of the rain intensity horizontal spatial distribution within the cell:

$$R(\rho) = R_M e^{-\frac{\rho}{\rho_0}} \tag{2.8}$$

ρ is the distance from the cell center, where the peak R_M is located, and ρ_0 is the equivalent radius of the cell, where $R(\rho_0) = R_M/e$. The fundamental parameters that entirely describe the rain profile are R_M and ρ_0 and during the scene can evolve. For this reason the equation (2.8) must be rewritten in function of t

$$R(\rho, t) = R_M(t) e^{-\frac{\rho}{\rho_0(t)}} \tag{2.9}$$

The evolution of R_M is modeled with an exponential curve described in detail below, as for ρ_0, considering the theory about the joint evolution of the peak rain rate R_M and of the equivalent radius ρ_0 proposed in the same work and pointed out by the study of the evolution of 742 cells in the NPC database [4]. In this section, after a description of the theory utilized, will be explained how this theory is been applied in the simulator.

2.3.1 Rain rate peak evolution

In the application the cell can evolve during its movement and its dynamicity is given by the evolution of the parameters R_M and ρ_0.
The theory to describe this evolution is supplied by a previous study on 742 rain cells thresholded at $5mm/h$ extracted from the NPC database.
Every cell was associated to the corresponding R_M and ρ_0 values, which descend from the preservation of the area and of the mean rain rate of the real cell.
The time evolution of $R_M^i(t)$, with i the i-th cell, was normalized to its peak value $R_{M,p}^i = arg\max\{R_M^i(t)\}$ and time shifted in order to make $R_{M,p}^i$ corresponding to $t = 0$.
Regardless of the rain cell intensity and of the time at which the maximum value of R_M occurs, the overall trend of R_M with time was investigated.
It turned out that the time history of $R_M^i(t)$ is well approximated by the following exponential law:

$$R_{M,n}^i(t) = R_M^i(t)/R_{M,p}^i = e^{a|t|} \tag{2.10}$$

$R_{M,n}^i$ represents the normalized evolution of the peak raint rate R_M of the i-th cell with respect to the maximum peak $R_{M,p}$ that it can reach.
In the next figure is presented an example of the evolution of the peak rain rate of a set of cells $R_M^i(t)$.

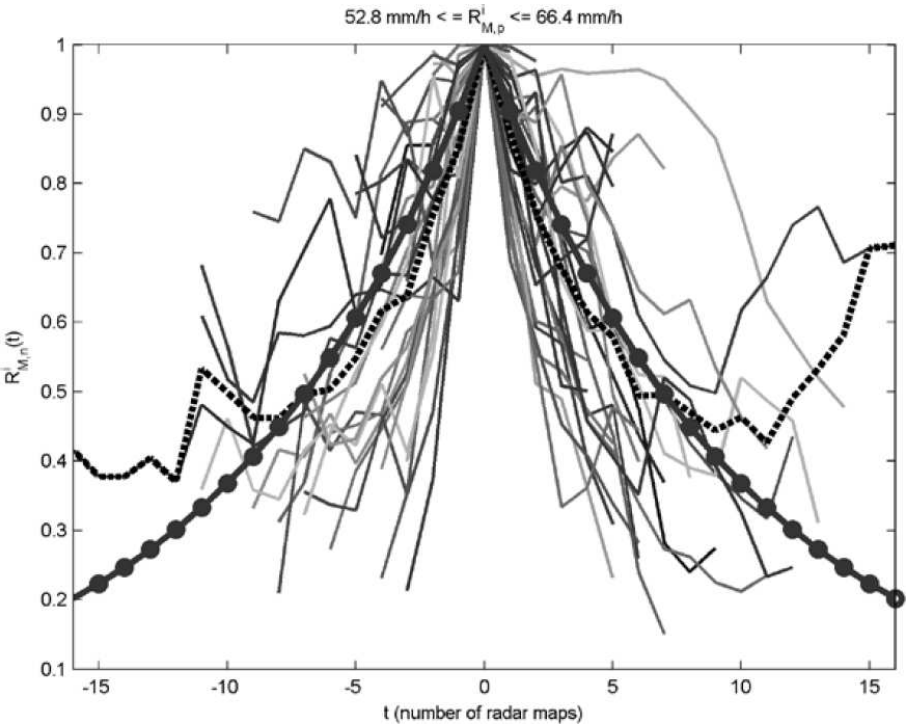

Figure 2.5: Example of R_M evolution. $R^i_{M,n}(t)$ evolutions pertaining to the class $52.8mm/h \leq R^i_{M,p} \leq 66.4mm/h$: the black dashed line indicates the average trend, the grey line with circles is the exponential fitting law, for which $a = -0.1$.

The original information of $R^i_{M,p}$ was used to classify the evolutions into 20 logarithmic intervals of $R^i_{M,p}$, defined according to the lowest and the highest values found in the database, respectively equal to 6.7 mm/h and 656.9 mm/h. This classification was made realizing that the decrease of equation (2.8) with t is steeper as $R^i_{M,p}$ increases and therefore it need to determine the parameter a for each class, which is representative, on the average, of all the evolutions pertaining to that class.
The trend of a with rispect to $\overline{R}^c_{M,p}$, the geometric mean of the cell in the database for a given class c, is reported in Fig. 2.6: it is shown that a tends to decrease with increasing $R^c_{M,p}$.
This result underlines that it is very likely that the most intense cells tends to reduce more rapidly than those one less intense. As a first approximation, a values reported in Fig. 2.6 can be fitted by a power law (indicated by the grey line with circles), whose expression is

$$a = -0.024(\overline{R}_{M,p})^{0.299} \tag{2.11}$$

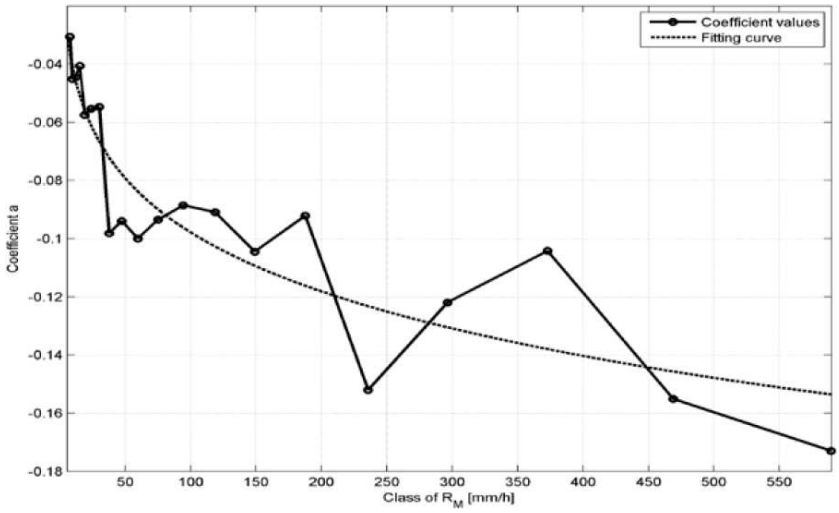

Figure 2.6: Trend of coefficients a in equation 2.11 for each class of rain cell's evolution.

2.3.2 Hyperbolic relation between the peak rain rate and the equivalent radius

As it is clear from the the scatter plot represented in Fig. 2.7, R_M and ρ_0 appear to be negatively correlated and their relationship is very well described by the following hyperbolic expression:

$$R_M(t) = k/\rho_0(t) \tag{2.12}$$

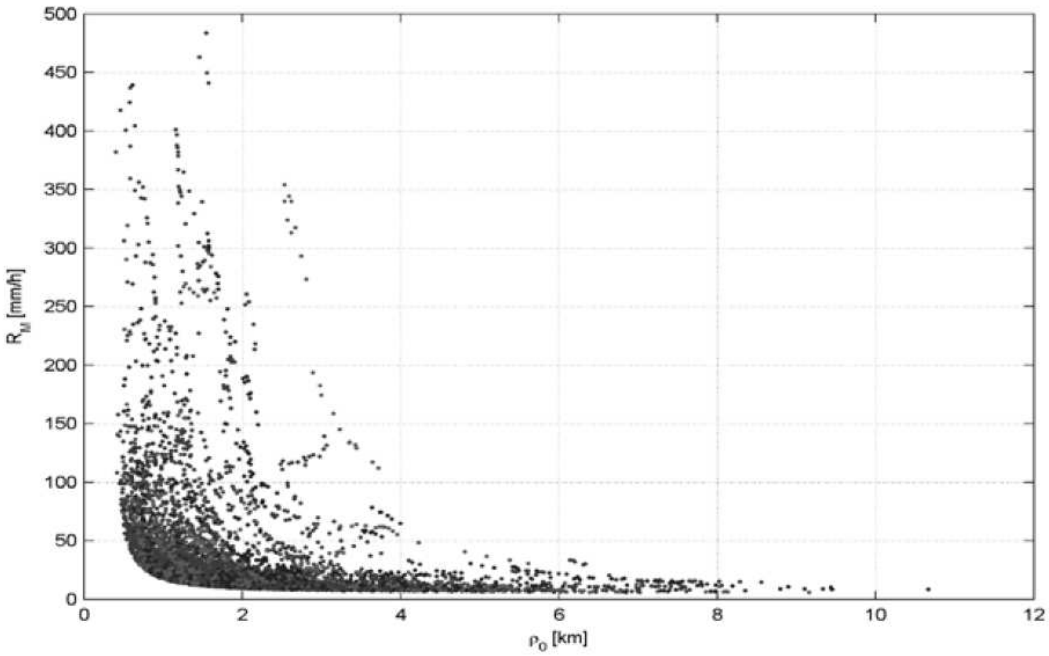

Figure 2.7: Scatter plot of the joint evolution of R_M and ρ_0 through the hyperbolic model in equation.

Equation (2.12) defines a sort of "pulsating cell": when the peak intensity of the cell increases (R_M), its spatial extent (ρ_0) reduces, whereas, on the contrary, when the cell becomes less intense, it widens and tends to assume a flatter shape. Moreover, the trend expressed by equation (2.12) is simple as the initial state of a synthetic cell (i.e., a set of R_M^* and ρ_0^* values) is sufficient to determine the parameter k, and, thus, to completely define the cell's temporal evolution [4]. In addition, the hyperbolic model is also very accurate as it can be deduced from Fig. 2.8 where are plotted the hyperbolas fitting the temporal evolution of all the 742 tracked cells.

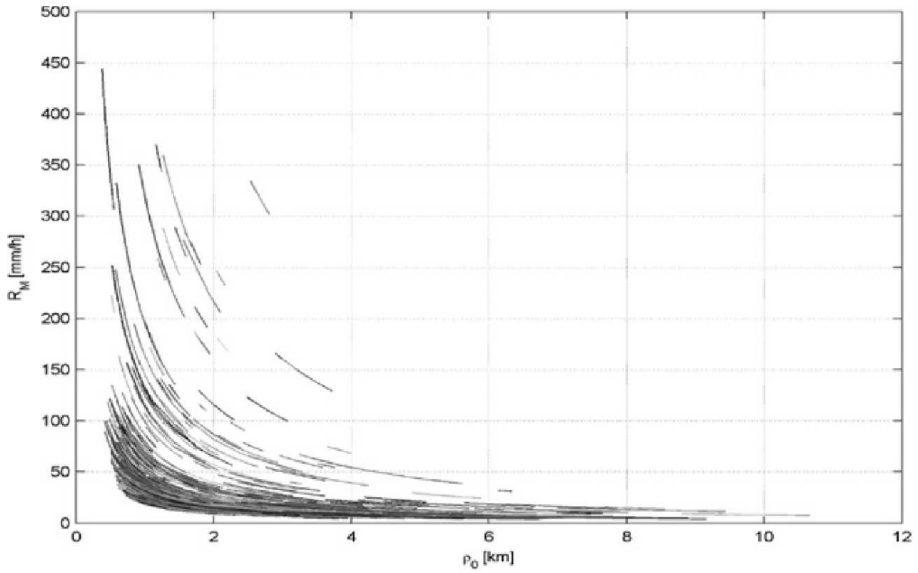

Figure 2.8: Fitting of the joint evolution of R_M and ρ_0 through the hyperbolic model in equation (2.12).

The k parameter is chosen in function of the probability of occurrence $N(R_M, \rho_0)$ of a determined cell. In previous works it is noticed that it is possible setting to zero the probability of occurrence of the cells for a given couple of (R_M, ρ_0) with probability less than $2.3 \cdot 10^{-7}$, committing a negligible error [3]. Probability of occurrence are been classified within a matrix divided in linear intervals for ρ_0 and in logarithmic intervals for R_M . After the elimination of the occurrence with probability less than $2.3 \cdot 10^{-7}$ in the matrix remain curves with ρ_0 spread in the range of 0.5 km to 12km and R_M in the range of 5 mm/h to 700mm/h. For this reason k can be chosen in the range of 2.5 to 1400.

In the simulator, referring to a random i-th cell, the user can choose a $R_{M,p}$, the geometric mean $\overline{R}_{M,p}$ and the parameter k. These values are used to generate the curve of the R_M evolution plotted in Fig. 2.5. In a random manner the program choose an initial point on the curve, generate a set of directions that R_M will follow along the curve and build the history for R_M. At the end of this procedure the program calculate an array containing the values of the final curve for R_M and another one, calculated by means of k, containing the corresponding evolution for ρ_0.
In Fig. 2.9 is reported an example of the curves generated with the algorithm: on the top the main curve built by means of the expression $R_M(t) = R_p exp(a|t|)$ (from now on $R_{M,p}$ is called R_p) and time shifted after 0; the green arrows represent the random direction (the number on the arrows indicates the order of generation) that connect the portions on the curve utilized to generate the his-

tory of the evolution of R_M used during the scene and presented in the figure on the bottom. $\overline{R}_{M,p}$, for each example here presented, will be the geometric mean between the lower and the higher values of the c interval to which R_p belongs.

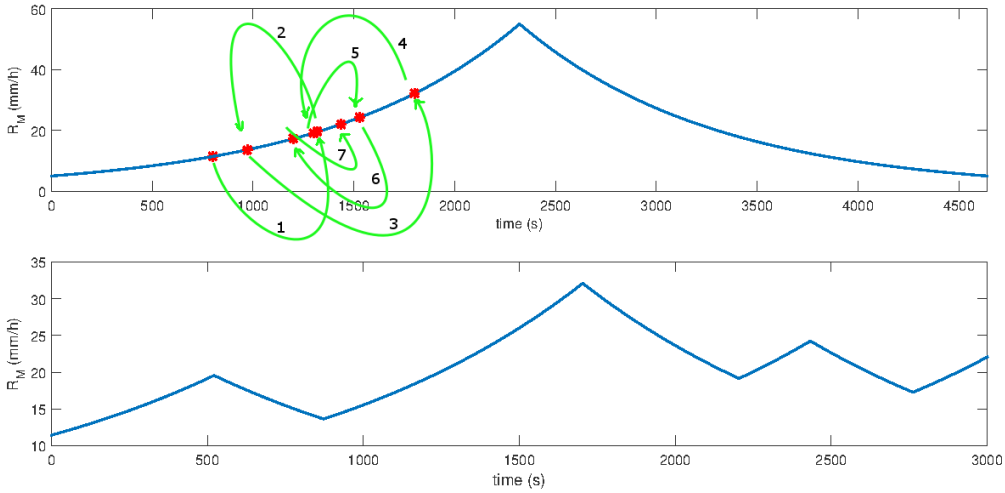

Figure 2.9: Example of generated curve for the evolution of the peak rain rate of the cell R_M with $R_p = 55$ for a history of 3000 s.

2.4 Simulation

Once defined every parameters of the cell the simulation starts by repeating every time step n with n=0,1,2...$\lceil T/T_s \rceil$ the following two steps:

1. To generate the EXCELL profile is necessary have a matrix big enough to contain the entire cell with a given threshold (usually 5mm/h), which value is given by the maximum radius of the biggest cell we want to represent, chosen equal to 50km (upper limit [4]) . The dimension in pixel of the matrix containing this cell is related on the resolution selected. Given the initial couple R_M, ρ_0, a function sets the value 0 in the center of the matrix and the values of surrounding pixel are given by the euclidean distance from that central pixel. Every value of the matrix will be recalculated with the expression 2.8 with ρ the distance within the matrix; those values below the rain threshold will be set to zero. Finally, this matrix is positioned within the map matrix at the coordinates $x(nT_s)$, $y(nT_s)$ determined by the position where they should be in the map at time nT_s.

2. The rain attenuation A (dB) suffered from the radio link of the rainy path length L is calculated as

$$A = \int_0^L \gamma_R(l)dl = \int_0^L kR(l)^\alpha dl \tag{2.13}$$

Finally, another parameter not defined by the user and dependent only on which precision is necessary to best represent the attenuation is the sampling step of the radio link L_{slant}, useful to calculate the attenuation in points where the pixel of the matrix could be only partially occluded by the link.

This expression is evaluated as a summation of specific attenuation suffered by the points of the link defined with sampling step L_{slant} with which the link is discretized.

All the 3D points of the link are projected to the ground and define a set of coordinates x,y rounded to the nearest integer within the matrix of the map corresponding on the indexes of the matrix touched. This set of indexes is then used to find out which values of the matrix of the rain rate don't present a significative value (different by zero): this index will not used in the calculation of the attenuation and therefore it will discarded.

Any link's portions L_{slant} has a resolution on the ground ΔL that is projected along the slant path calculated in function of the angle between the transmitter and the receiver: it is the ration between the resolution on the ground and the cosine of the angle θ

$$L_{slant} = \Delta L / cos(\theta) \tag{2.14}$$

It is then defined the array W that can assume two values:

$$W = \begin{cases} L_{slant} & \text{if } x \leq H \\ 0 & \text{if } x > H \end{cases} \tag{2.15}$$

The value of W indicates that each portion of link affected by rain with length L_{slant} gives a contribution to the attenuation equal to the product between the specific attenuation, calculated with the expression (2.4) in the corresponding pixel on the ground, and L_{slant}. The weight for the points of the link above the height of the rain are set to zero.
A schematic representation of this operation, that shows the link affected by rain and its corresponding points that are used in the calculus of attenuation, is presented in Fig. 2.10. The green line represents the link's portion not affected by rain, the red line the one affected and the black line the portion of link above the height of the rain. The cell is the filled light blue circle, the height of the rain cell is 3.5km and the link represents a

communication between two points (blue circles): one positioned 10m a.s.l (right bottom corner) the other (left top corner) at 4300m a.s.l.

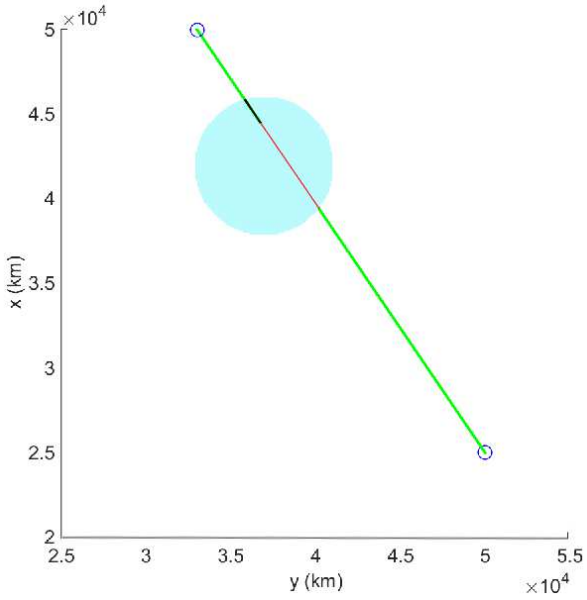

Figure 2.10: Schematic representation of the parts of the link affected by rain used in the calculus of the attenuation.

It is possible now translate the equation (2.13) in discrete terms by means of the expression:

$$A = \sum_{i=0}^{N} k(R_i W)^{\alpha} \tag{2.16}$$

with i the index of all 3D discrete points which number is $N = \lceil L_E / L_{slant} \rceil$.

2.5 Examples

With this simulator it is possible to obtain several configurations varying the input parameters as the position of the cell with respect to the link, height of the rain, speed of the cell, or changing the parameters for the evolution of the dynamic cell as R_M, k or R_p.
Example of the more meaningful possible scenarios are shown in the pictures below, where the scene are sampled every 200s.

2.5.1 Simple evolution of dynamic cell and calculus of the attenuation

In this example is shown a dynamic cell that is moving in a portion of the map and evolves during the scene follow the exponential curve described in (2.10). The link is between two station positioned on the ground and during the scene is always affected by rain.
The cell starts with a low R_M (about 7mm/h) and then grows. The decreasing of the attenuation at about 700s is given by the shrinking of the cell and, hence, the calculus of the attenuation along the side, where the values of rain rate are relatively low. The peak R_M of the cell at 1500s reaches the top of its evolution: at this moment the cell is reduced of about 6 times with respect to the starting point and the attenuation is maximum. Finally, the attenuation decreases showing a behavior similar to the first part of the evolution, it increases or decreases in function of the dimensions of the cell that occupies the link and of the position of the link with respect to the maximum where attenuation increases as shown in Fig. 2.13 between 2500 s and 3000 s

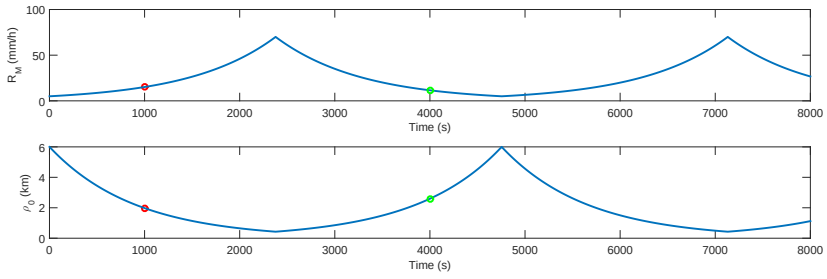

Figure 2.11: Sample of evolution for R_M (above) and the corresponding variation of ρ_0 (below) for a cell with $R_p = 70$ and $k = 30$.

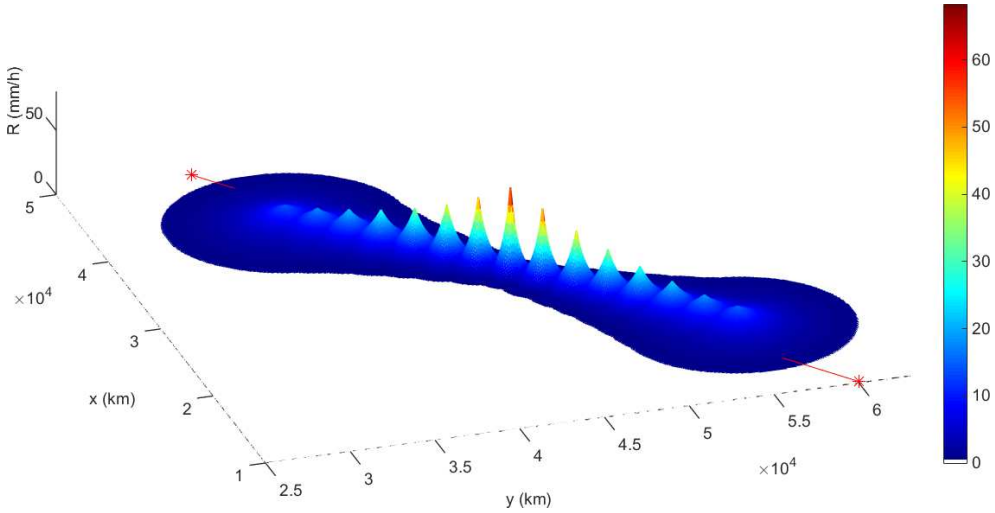

Figure 2.12: 3D representation of the movement and the profile evolution for a terrestrial communication with snapshots effectuated every 400 s, speed=10.6m/s.

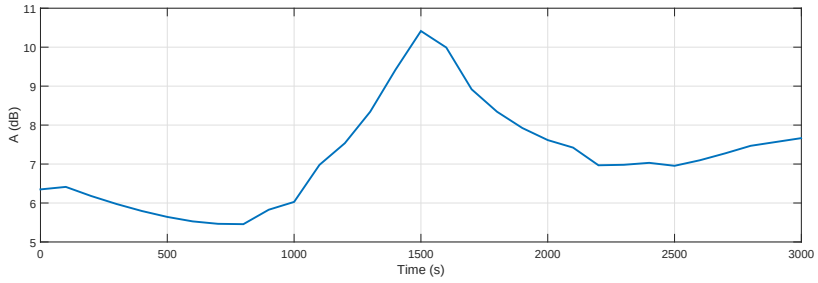

Figure 2.13: Attenuation experienced by the link, sampled every 100 s.

2.5.2 Attenuation for a link partially affected by rain

In this second example it is shown a link that at a certain moment is above the height of the rain. In this example it is increased the dynamicity of the rain peak R_M. The attenuation remain low because the link is not in proximity of the center of the cell and the peak is relatively low in the beginning of the scene. As soon as R_M tends to become bigger, around t=3500 s, the link is positioned in the way such that it exits above the height of the rain cell; this it reflects on a steeper decreasing of the attenuation to zero.

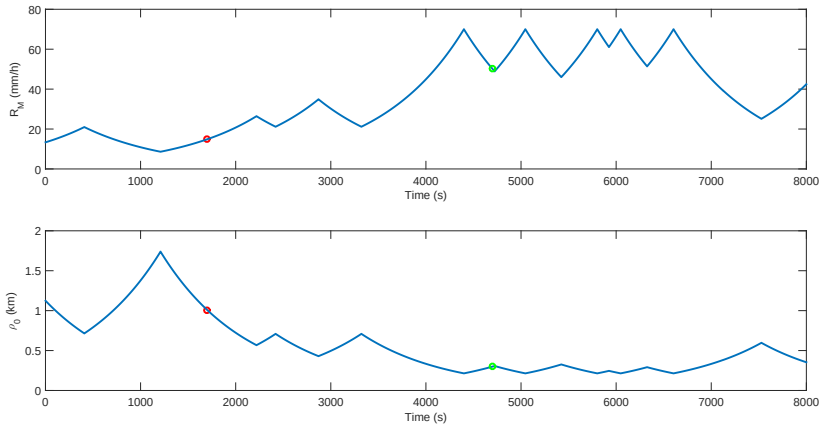

Figure 2.14: Sample of random evolution for R_M (above) and the corresponding variation of ρ_0 (below) for a cell with $R_p = 70$ and $k = 30$.

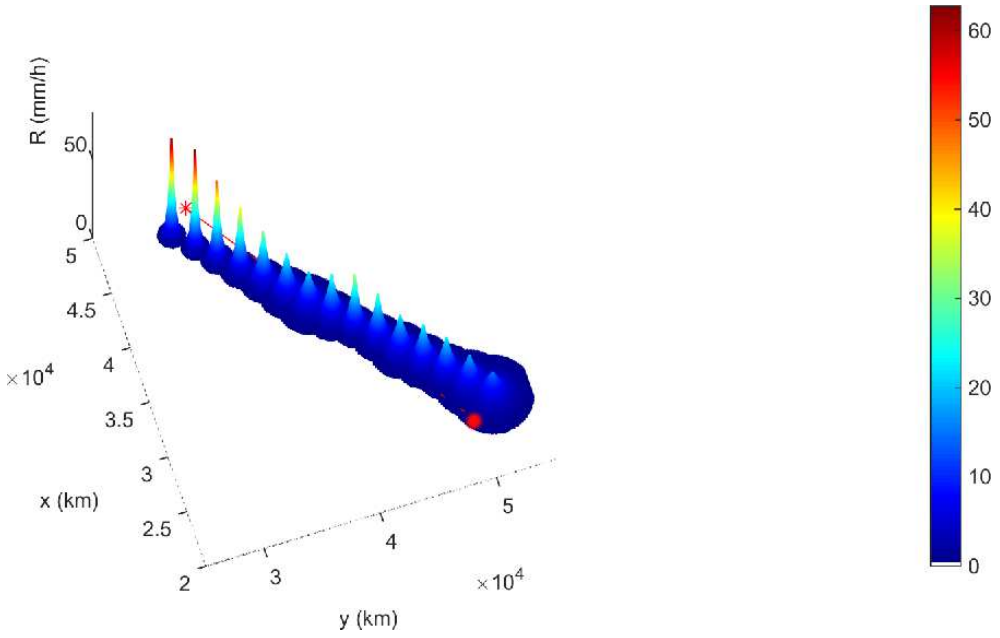

Figure 2.15: 3D representation of the movement and the profile evolution of a dynamic, with snapshots effectuated every 400 s, speed=10.6m/s.

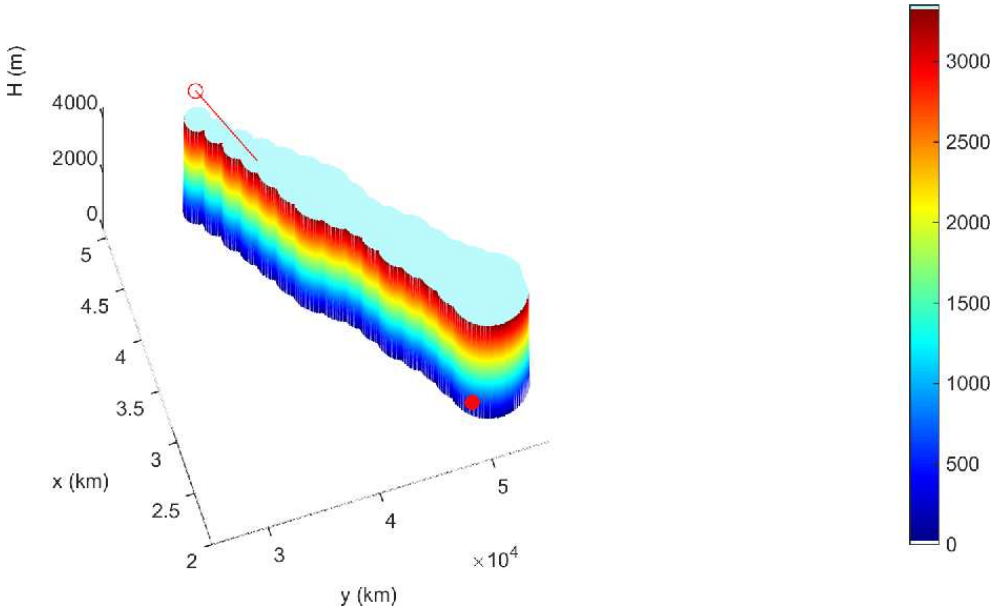

Figure 2.16: 3D representation of the movement and the height of the cell (H=3.35km), for a terrestrial communication with snapshots effectuated every 400 s.

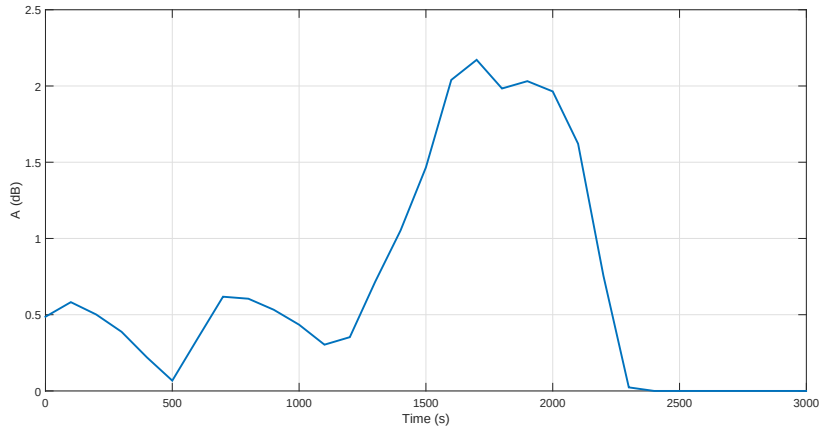

Figure 2.17: Attenuation experienced by the link, sampled every 100 s.

2.5.3 Comparison between static cell and dynamic cell

In this example it is shown the difference between the attenuation calculated utilizing a static cell and a dynamic cell for a link between two divices, the former

at 1 m a.s.l, the latter at 44 km a.s.l. Both the cells start with the same R_M and ρ_0, but while the former maintains the same shape during the scene, the latter evolves along the curve of R_M. The cell moves along the link: this particular configuration led to have the maximum attenuation possibile for this type of cell because it completely covers the link while it passes through the center. As we can see the initial attenuation is the same, the change of shape reflects in a consequent evolution of the attenuation. In this case the link is not always affected by rain because for t=2300 s the link is above the height of the rain cell.

Dynamic Cell

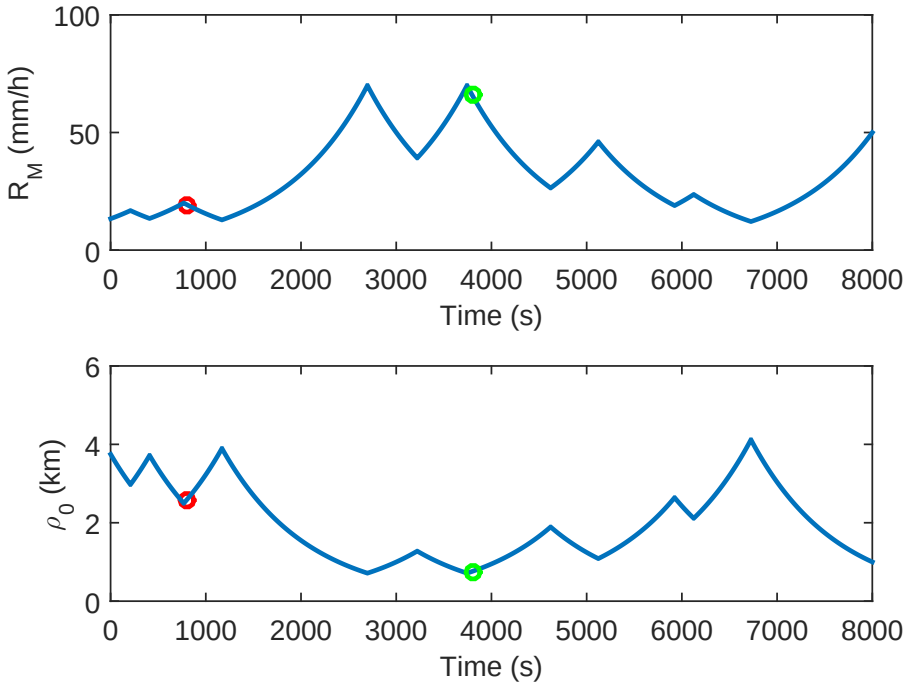

Figure 2.18: Sample of random evolution for R_M (above) and the corrisponding variation of ρ_0 (below) for a cell with $R_p = 70$ and $k = 30$.

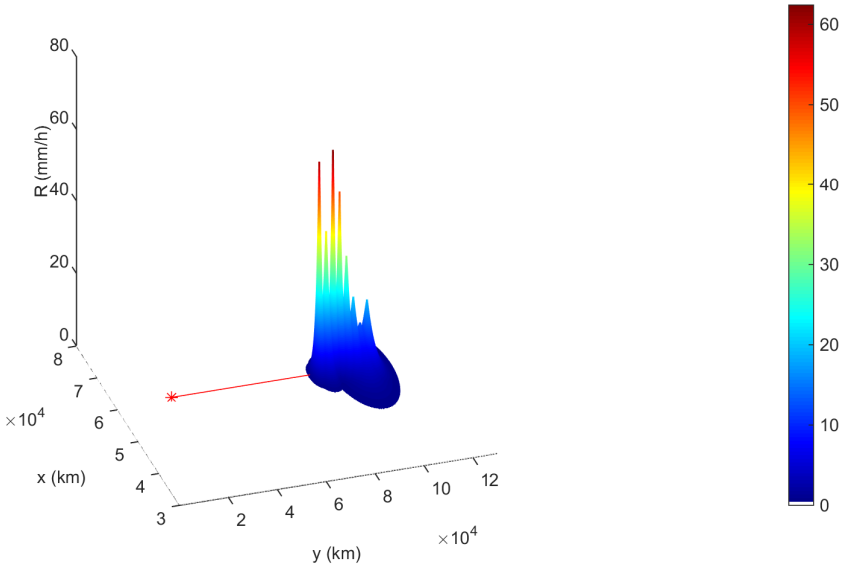

Figure 2.19: 3D representation of the movement and the profile evolution of a dynamic cell for a spatial communication with snapshots effectuated every 400 s and translation velocity equal to 6.95 m/s.

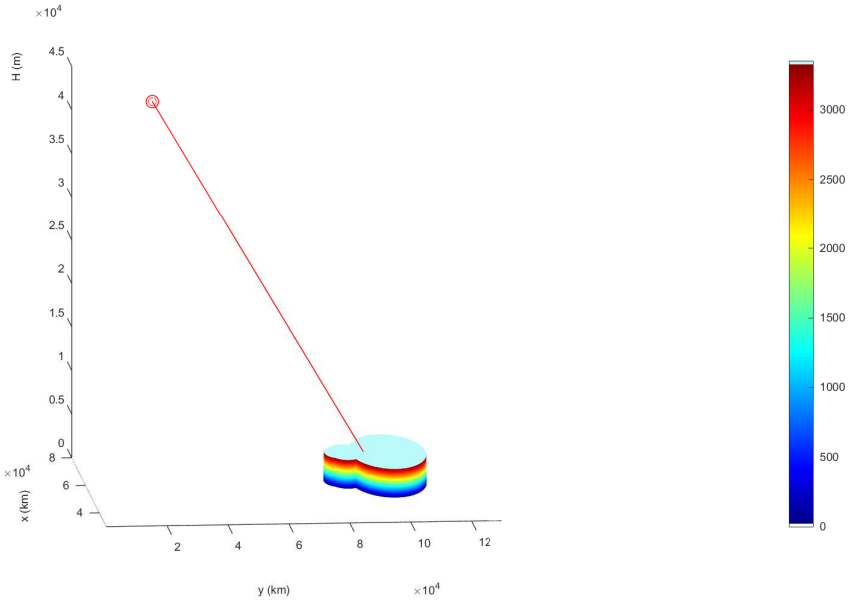

Figure 2.20: 3D representation of the movement and the height (H=3.35km) of a dynamic cell for a spatial communication with snapshots effectuated every 400 s.

Static Cell

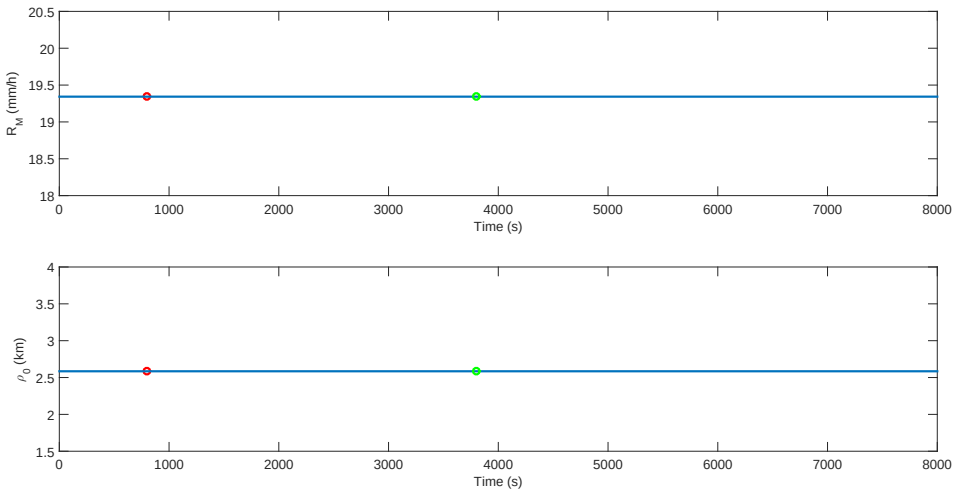

Figure 2.21: Representation of the values of R_M and ρ_0 maintained by the cell during the scene.

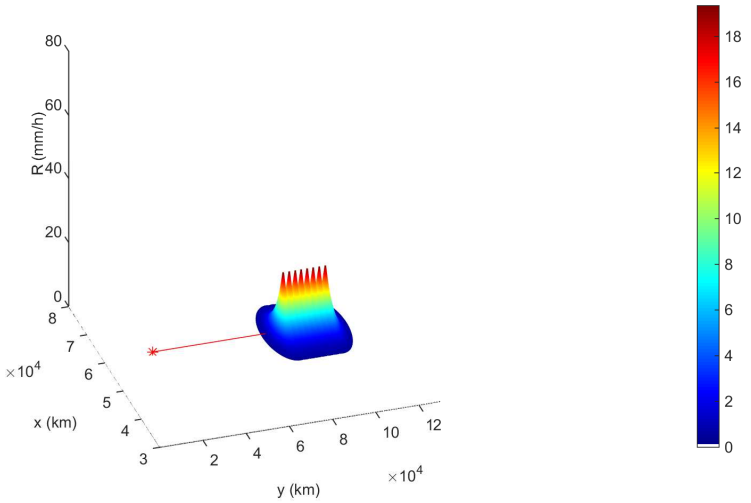

Figure 2.22: 3D representation of the movement and of the profile for a static cell for a spatial communication with snapshots effectuated every 400 s.

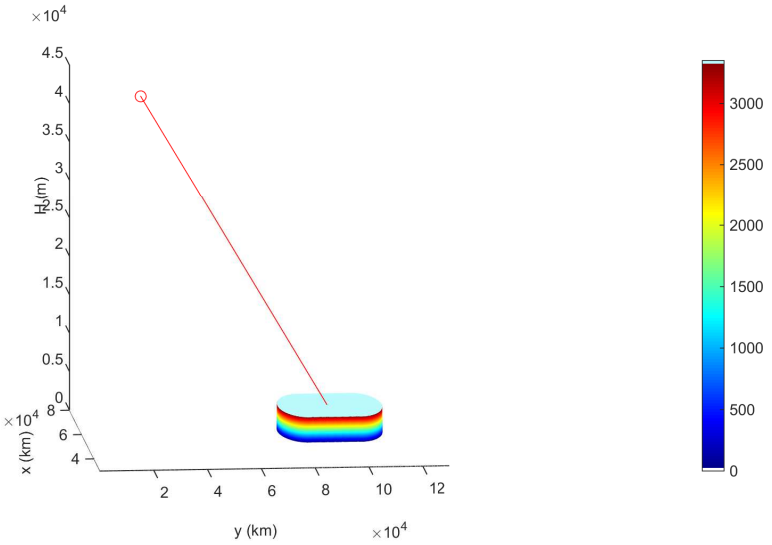

Figure 2.23: 3D representation of the movement and the height of a static cell for a spatial communication with snapshots effectuated every 400 s.

Comparison of attenuation

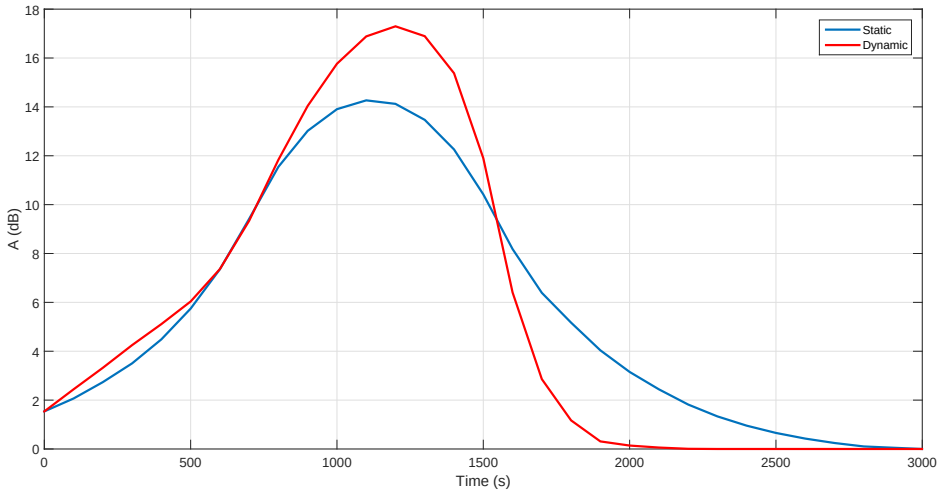

Figure 2.24: Comparison between the attenuation due to the dynamic cell and the static one.

Chapter 3

Multi EXCELL

The characteristics of the weather rain maps immediately points out that rain cells are not random distributed in space, but rather, they tend to aggregate to form larger structures [11] as shown in Fig. 3.1. These characteristics led to the study of three classes of rainfall spatial correlation:

1. the small-scale correlation (up to approximately 20 km) tightly linked to the horizontal spatial distribution of the single rain cells that can be modeled by means of the EXCELL.

2. the mid-scale correlation (ranging roughly from 20 km to 50 km) that depends on how cells cluster to form an aggregate and how cells interact among them, identified in Fig. 3.1 by red lines.

3. the large-scale correlation (from 50 km to about 300 km) which is connected to the mutual position of the large aggregates and can be a composition of more cells identified in Fig. 3.1 with green lines.

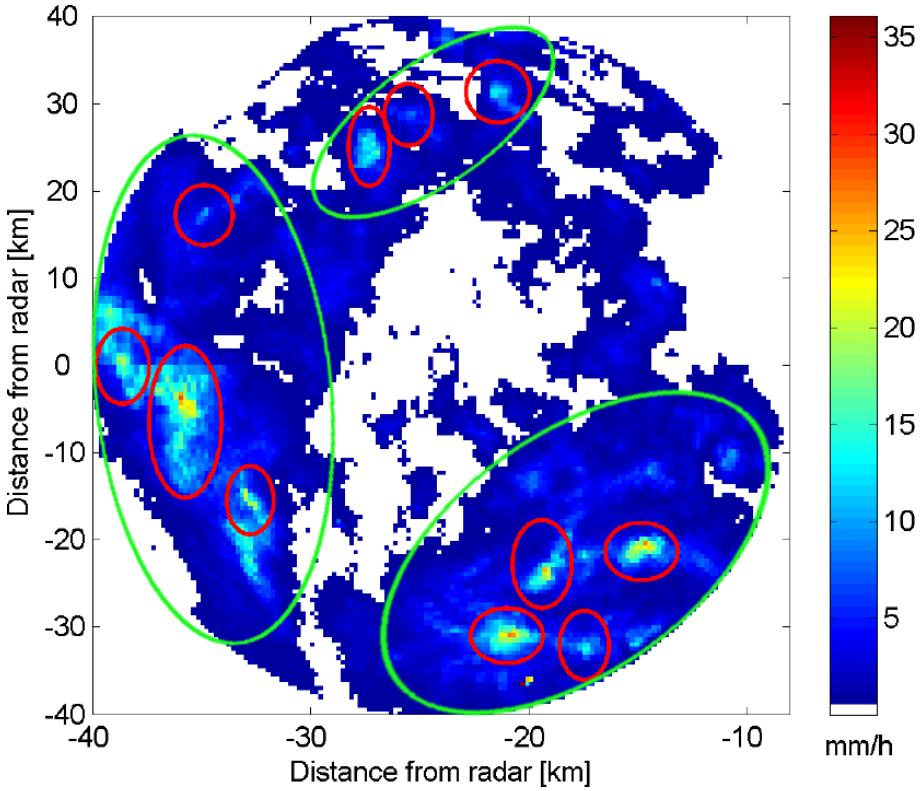

Figure 3.1: Typical rain field (in mm/h) measured by the weather radar located at Spino d'Adda, positioned in the center of the map; some rain cells are roughly identified by red ellipses while the aggregated are identified by green lines.

Some applications, such as the prediction of the attenuation experienced by an Earth-space communication link described in the previous chapter, involve a single rain cell at a time; on the contrary, other applications require the simulation of the complete rain field. This is the case, for instance, of *site diversity systems*, whose performance, depends on the rainfall spatial variability also at large scale. The same is true for *time diversity systems*, for which the retransmission of the same piece of information after a suitable time delay T strongly reduces the probability that both at t and t+T the system is undergoing an outage. When T increases, it is very likely that more than one cell will interact with the transmission link. In this chapter we describe the behaviors of the evolution of the principal descriptors of a number of EXCELLs within one or more aggregates applying the theory explained in Chapter 1 and using the dynamic characteristics of the evolution of the rain peak showed in Chapter 2.

3.1 Fractional rainy area

The knowledge of the area of a map covered by rain is of fundamental importance for the generation of realistic rain fields. In fact, the spatial correlation of the rain intensity is tightly linked to the rainy area: a limited coverage implies a steep decrease of the correlation with distance, whereas the opposite is true for rain fields characterized by a wide coverage. In the literature, this subject has been investigated in terms of fractional rainy area, η, defined as the ratio between the portion of the observation area covered by rain, A_R, and the total area considered [11]:

$$\eta = \frac{A_R}{A} \tag{3.1}$$

The distribution of the fractional rainy area and the evolution over time depends on the local climatology: it is expected to show a seasonal variation, according to the fact that, especially in temperate areas, precipitations tend to be mainly stratiform or mainly convective during winter or summer months, respectively. Furthermore, it also tends to be larger in sites where mainly stratiform phenomena (characterized by a mean rain rate smaller than 5 mm/h but a larger covered area) occur compared to the sites where the convective events prevail.
As it can be observed in Fig. 3.2 the fractional coverage η tends to be stable (or to decrease less) for a while and after that it decreases again [11]. This behavior has a physical explanation: at small A_R the analysis is focused on the mid scale, the number of rain cells considered in this area is low and as a consequence η is highly variable as it could be observed within a single aggregate. This is not true instead when the observed area corresponds to the whole map where the velocity evolution of η is overall reduced.

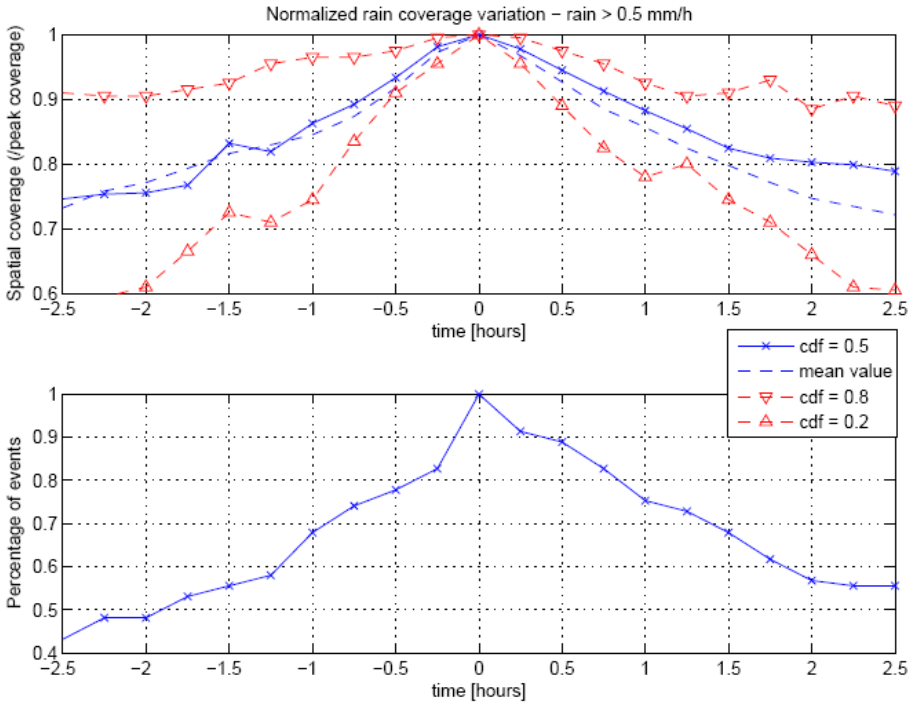

Figure 3.2: Fractional of the rainy area evolution for a rain threshold of 0.5mm/m. The mean value is represented by the blue line, the red line represent 20 and 80 percentiles, respectively.

The evolution of the fractional rainy area refers to the work effectuated on the radar images collected at Spino d'Adda from 1988 to 1992 for a total of 81 rain events. After having normalized the fractional coverage of every events to the maximum value and shifted their time axis so to make the peak coincide to the arbitrary time equal to 0 h, they were analyzed. The work pointed out that, as shown in Fig. 3.2, for a threshold value of rain rate of 0.5 mm/h, the average variation of the fractional coverage is relatively limited: within 15% in 1 hour time and increases slowly to 30% after 3 hours. In the figure above is plotted also the 20 and 80 percentiles as well as the median value confirming what stated before.
In this work it is considered that a small variation of the fractional coverage reflects in a corresponding small variation of the water quantity $Q = \overline{R} \cdot A$ $[mm/h \cdot m^2]$ described in Chapter 1.

3.2 Aggregate evolution

In this work, to adapt the algorithm to the values above mentioned, the fractional rainy area η is chosen between a possible curve within the 20 and 80 percentile. This choice permits also to observe different behaviors having curves with gradients more or less far from the mean curve. Moreover, observing the majority of the events, it has been deduced that the curve of η follows a linear trend during the scene, starting with a certain value, it reaches a maximum and then decreases.

With these considerations in mind the curve of the fractional rainy area of the map is generated with this procedure:

1. Calculation of the first value between 20 and 80 percentile of the local fractional area evolution curve, that is a value included between -30% and +30% with respect to the mean value represented by the blue curve in Fig. 3.2;

2. The maximum is fixed to 1 at the center of the total time window since the entire curve is normalized to the peak value of η;

3. Calculation of the last value between 20 and 80 percentile for the local fractional area evolution curve.

The values generated with this procedure are then spread over a large time window chosen at the beginning of the simulation (for example, 18000 seconds, about 5 hours to match with what reported in Fig. 3.2), by means of a linear interpolation.
An example of generation of the evolution of the water quantity of the map is shown in the following figure. Comparing the curve with the one in Fig. 3.3 can be noticed that it lies between the two red curves that limit the possible value of this curve.

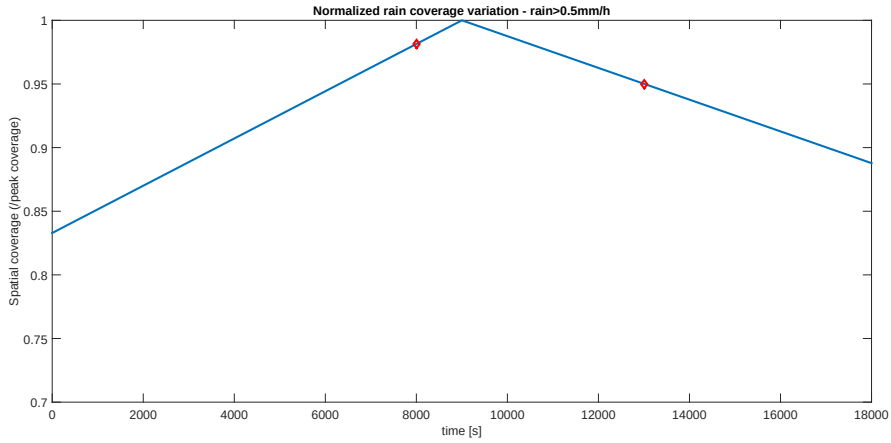

Figure 3.3: Evolution of percentual rainy coverage generated by the algorithm.

Once generated the curve it is possible to choose the time window to analyze the evolution of the aggregate as shown in Fig. 3.3. The starting point of the window corresponds to the initial value of the total water quantity of a map: this choice is related to the fact that we know the water quantity at a given time but we have to know in which moment the water quantity is observed, for example if it is observed when the event is just started, and hence when the quantity of water is increasing, or when the rain event is almost finished and the water quantity is decreasing.
To calculate the initial value of Q_i, $Q_i(0)$, with i index of the aggregate, is necessary having the couple (R_M,ρ_0) for every cells pertaining to the aggregate i and calculate their water quantity by means of this expression [5]:

$$Q = 2\pi\rho_0^2 R_M[1 - (R_{th}/R_M)(1 + ln(R_M/R_{th}))] \tag{3.2}$$

with $R_M \geq 5mm/h$ and $R_{th} = 0.5mm/h$. The value of R_{th} is so chosen to have a match with the fractional rainy coverage previously generated. The i-th aggregate i is a composition of a number N_i of daughters; the summation of their water quantity $Q_{i,j}$, with j the j-th daughter pertaining to aggregate i, at the initial instant corresponds to the water quantity of the aggregate $Q_i(0)$ and it is calculated by the expression:

$$Q_i(0) = \sum_{j=1}^{N_i} Q_{i,j}(0) \tag{3.3}$$

During the scene evolution, the water quantity of the map will follow the percentual variation of the corresponding fraction rainy area of the map, and at time

t it will be

$$Q_{map}(t) = \frac{Q_{map}(0)}{\eta(0)}\eta(t) \quad with \quad Q_{map}(0) = \sum_{i=1}^{N} Q_i(0) \tag{3.4}$$

whit N the number of the aggregates in the scene.
The evolution of water quantity for any aggregate can be calculated as a summation of N segments with different initial values, corresponding to the initial value $Q_i(0)$ previously calculated, and different speed variation. The initial time of analysis may result in 2 different cases: the case of one trend if the evolution is only increasing (for an analysis window chosen before the maximum and that doesn't include the maximum) or decreasing (for an analysis window chosen after the maximum and that doesn't include the maximum), or two trends if the evolution starts with a positive slope, reach the maximum and then decreases.
The first behavior implies a simple summation of N segments with different initial point and different slope (positive or negative), in particular, they are calculated utilizing this expression:

$$m_0 t + q_0 = (\sum_{i=1}^{N} m_i)t + \sum_{i=1}^{N} q_i \tag{3.5}$$

with m_0 the slope of the water quantity of the map in the time interval, q_0 the initial value and m_i and q_i random chosen. It is worth mentioning that, being the amount of water a positive quantity, the solutions for m_i and q_i that have negative values, are not phisically acceptable and they are discarded and recalculated. The possible high value of the slopes of different aggregates can be justified for aggregates belonging to stratiform or convective class of rainfall, with higher or slower incremental speeds, respectively.
An example of this first behavior is plotted in Fig. 3.4 while the corresponding two aggregates generated by the algorithm is presented in Fig. 3.5 and in Fig. 3.6

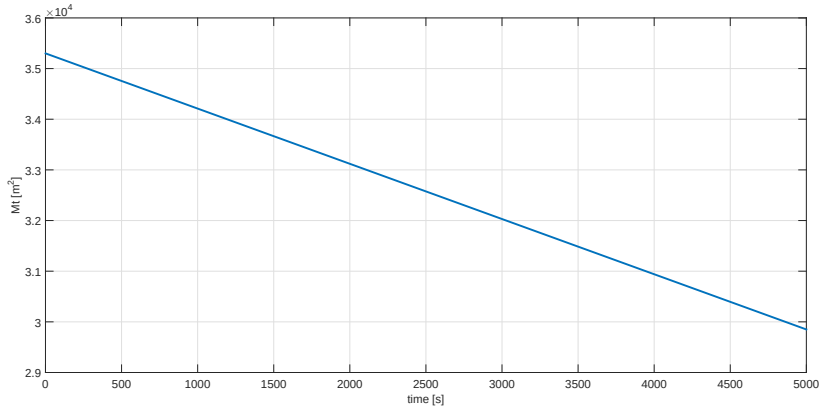

Figure 3.4: Evolution of the water quantity of the entire map for the first kind of behavior.

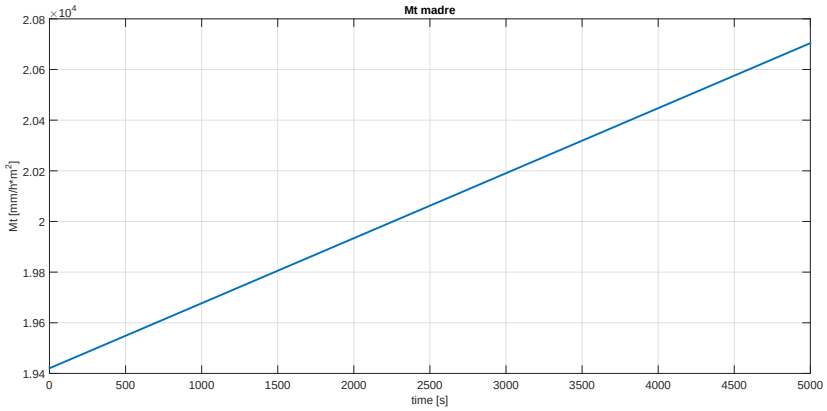

Figure 3.5: Evolution of the water quantity of Aggregate 1 for the first kind of behavior.

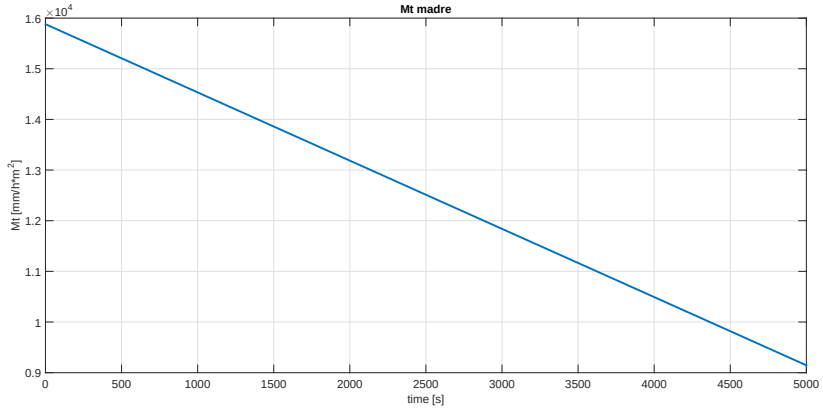

Figure 3.6: Evolution of the water quantity of Aggregate 2 for the first kind of behavior.

The second behavior, is handled finding the position of the maximum and then applying the same procedure utilized with the resolution of the equation (3.5). In this case, two casual segments will be calculated for every aggregates: one before the maximum and the other one after the maximum. The window analyzed for the water quantity of the map corresponding to the evolution of the spatial rainy coverage presented in Fig. 3.3, is reported in Fig. 3.7 and it is associated with two aggregates in Fig. 3.8 and 3.9 generated by the algorithm previously described for the second behavior.

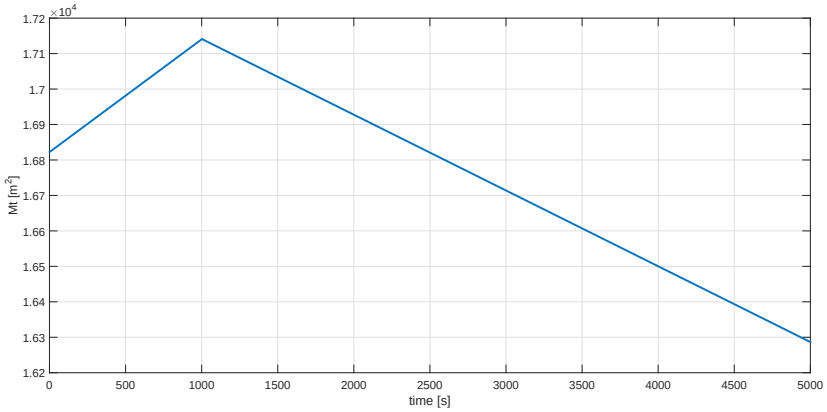

Figure 3.7: Evolution of the water quantity of the entire map for the second kind of behavior.

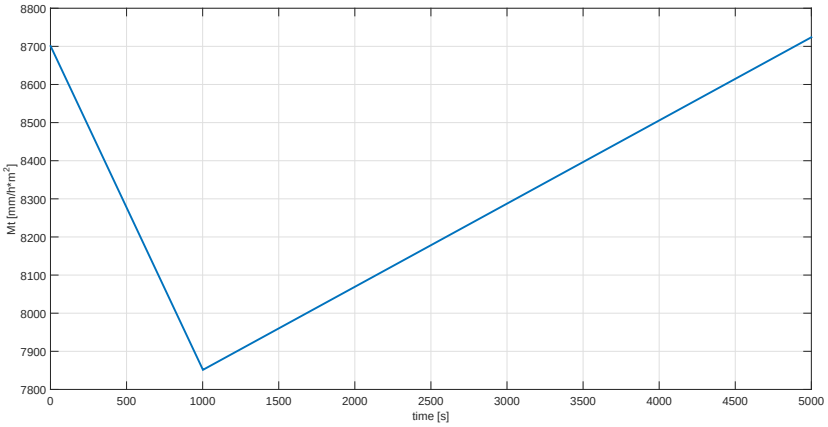

Figure 3.8: Evolution of the water quantity of Aggregate 1 for the second kind of behavior.

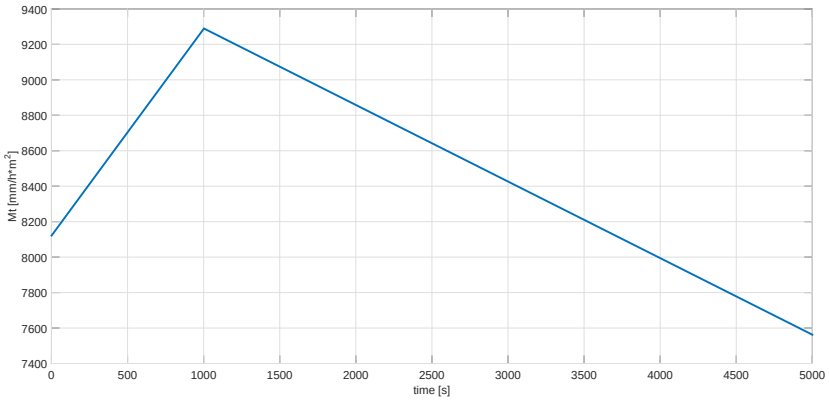

Figure 3.9: Evolution of the water quantity of Aggregate 2 for the second kind of behavior.

It is worth mentioning that for the rain structures the number of daughter cells must be properly chosen, for example, taking into account previous works carried out on LR maps in Spino d'Adda [4]. In this work the daughters are those cells with threshold $R > 5mm/h$ within aggregates defined for $R > 0.5mm/h$; it turned out that most of the aggregates consist of two daughters and very few of them have more than 25, as shown in the following figure.

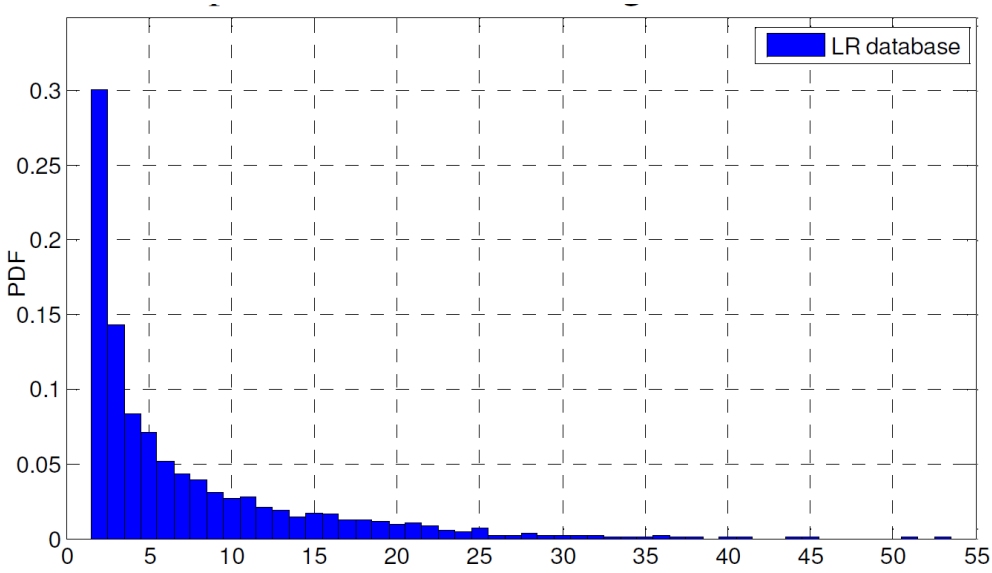

Figure 3.10: Probability density function of the number of daughter cells per aggregate.

3.3 Daughters' definition

Although the general definition of daughters cell establishes a threshold of $5mm/h$, in this section, to maintain the equality defined in expression (3.3), the synthetic

cells are defined with a threshold equal to $0.5mm/h$.
In the analysis of several rain events is turned out that the evolution of rain rate of the cells within the aggregate, that is the generator, called also "mother", is correlated with the evolution of the aggregate [12]. In particular, it was defined "prevailing" daughter the one having the largest area between all cells within the aggregate and it was observed the joint evolution of the parameters of that particular cell with respect to the parameters of the "mother" cell. In the next figure is shown an example of rain event where the evolution of the parameters of the synthesized cells are compared.

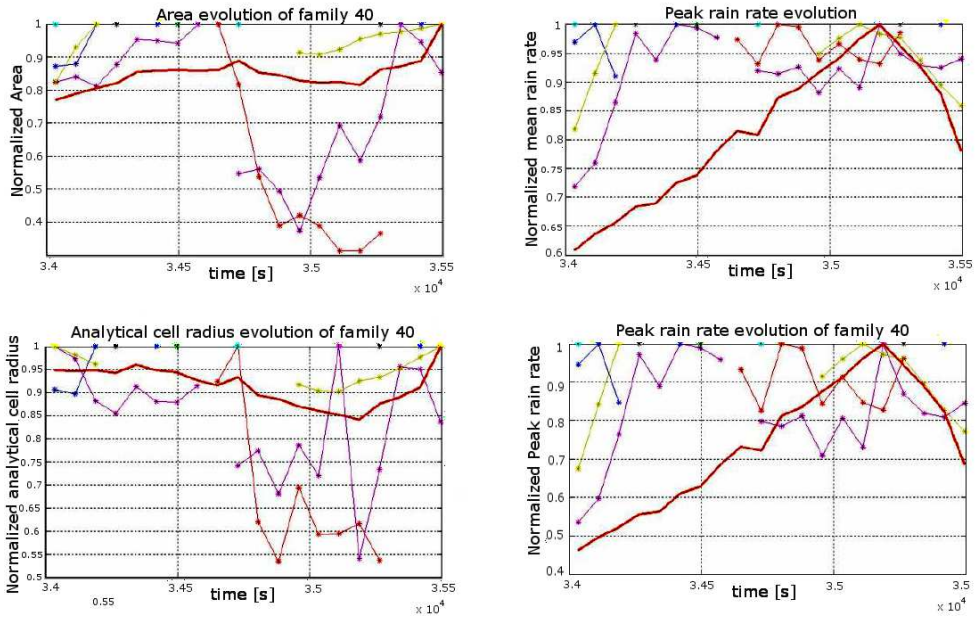

Figure 3.11: Time evolution of the normalized A, $\overline{R}$, ρ_0 and R_M for the family 40 from the 417 rain event. Observing after $t = 3.5 \cdot 10^4$ s it is noticed that all parameters of the Daughter cell (yellow line) evolve in the same manner of those pertaining to the mother (red line).

The analysis of the joint evolution of the generator cell and its "prevailing" 5 mm/h daughter cell reveals that the parameters of the daughter cell evolve mainly in the same manner as the ones of the mother cell. In this application the main daughter, at a given time, is identified as the one having the greatest water quantity over all the cell within the aggregate and is called "Driver daughter". The others cells are classified as "Secondary daughters" and their water quantity doesn't follow the trend of the mother.

3.4 Simulator

The evolution of the cells, represented by means of the EXCELL model, inside the aggregate is based on the trend of the water quantity Q_i. More specifically, the goal is to maintain the relations between the water quantity of the daughter cells and the water quantity of the mother during the evolution of the cells, simulating the behavior described above, where a "driver" daughter follows the trend of the mother while the others daughters have random behaviors.

3.4.1 Calculation of initial parameters

Another useful parameter for any cell is parameter $k = R_M \cdot \rho_0$ that relates the dimension of the cell with its rain intensity. In particular for any cell k is chosen based on the initial value of R_M and ρ_0, and it is maintained during the time window analyzed.
Every peak of the EXCELL R_M, as said in Chapter 2, have a typical time exponential evolution [4] given by the expression (2.10). The R_p parameter used in the expression (2.10) is fundamental to characterize the evolution of each cell and must be properly chosen to best represent the dynamicity of the cells and to maintain the correlation between the local P(R) and the probability of occurrence $N(R_M, \rho_0)$.
Moreover R_p is influenced from the characteristics of the rainfall, in particular the probability to have R_p high and therefore the possibility to a strong increasing with respect to initial value, is greater with respect to a uniform cell that maintains peak less intense and that shows a limited increasing from the initial instant.
Given R_p, different for each cells, the curve of the evolution of the peak rain rate is generated. The initial value of the peak rain rate given as input at the beginning of the scene is searched iteratively on the curve. The position on the curve at which the peak rain rate is best approximated is the starting point for the evolution of a given cell. At every peak rain rate is then associated the corresponding value of ρ_0.
This operation is well represented in Fig. 3.12 , that describes a scenario with the profile parameters of the cells listed in the following table.

Table 3.1: Example of initial parameters for a set of cells pertaining to the same aggregate and defined by R_p,initial R_M and corresponding ρ_0

#Cell	R_p $[mm/h]$	$R_M(0)$ $[mm/h]$	ρ_0 $[km]$
Rain cell 1	66	25	2.5
Rain cell 2	54	33	1.5
Rain cell 3	72	19	3

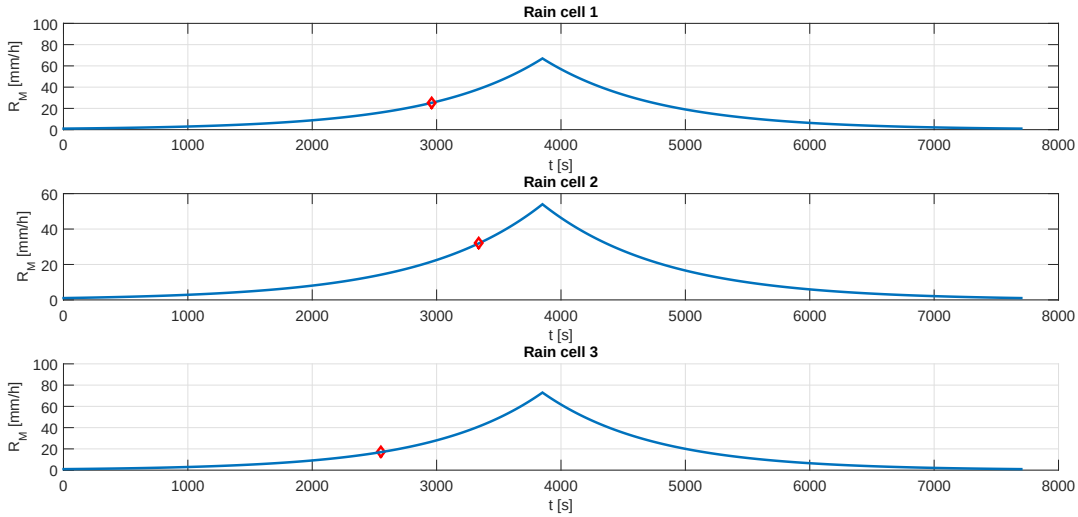

Figure 3.12: Sample of set of evolution curves for the peak rain rate for three different cell pertaining to the same aggregate. The red point for each cell represents initial value of its R_M along the curve.

3.4.2 Cells' evolution

During the evolution of the scene the following procedure will be applied for the daughters:

1. The direction of evolution of R_M followed is such that the water quantity of the driver cell Q_{driver} follow the trend of the aggregate.
2. Other daughters will follow a different direction of evolution for R_M are chosen so to be the best combination of the R_M in order to minimize the missing water quantity.

For this reason, the following relation applies:

$$Q_i(t) = Q_{driver}(t_{dr}) + \sum_{j=2}^{N_i} Q_j(t_j) \tag{3.6}$$

with j the index of secondary daughters. t_{dr} is the index along the curve of the rain peak evolution of the driver: it is updated with a new value chosen between

$(t_{dr}+1)$ or $(t_{dr}-1)$ based on which value of the new $Q_{driver}(t_{dr})$ follows the trend of $Q_i(t)$. t_j is the index along the curve of the rain peak evolution of the j-th Secondary Daughter. Each combination of (t_j+1) and (t_j-1) for all the set of Secondary daughters are tested in order to minimize the error of the water quantity remaining (the difference between water quantity of the map and water quantity of the aggregate). t_j for each Secondary cell is updated with the new value along the curve.
It is observed that an exponential evolution of R_M leads to an exponential evolution of Q_j. This behavior is quite annoying because Q_i presents a linear evolution and the expression above mentioned (3.6) represents a sum of functions, with order greater than the one of the exponential function, that would lead to higher values after a certain period, certainly exceeding the water quantity of the aggregate. This problem is noticeable only for the Driver cell since it is the only cell that must follow the trend of the aggregate for a long period. To linearize the trend, the lecture along the curve of R_M for the Driver cell is slower than the one of the other daughters.

3.4.3 Cells' exchange

When, during their evolution, the Q of a secondary daughter reaches the level of Q_{driver} it is promoted to driver cell, while the old driver daughter becomes a new secondary daughter.
It is noticed that sometimes the evolution presents a stall situation where daughters compete to effectuate the exchange. This situation is evident and must be corrected making any new exchange after a certain period. The choice of this time must be appropriate, in order to have fewer exchanges and to give the possibility to the driver to evolve more freely by increasing its dynamicity. A too long period could lead to loose the definition of "Diver cell" since the secondary daughter cell, that should do the exchange, would have a water quantity higher than that of the driver. In particular having an exponential evolution it would quickly lead to have the sum of water quantity of the cells exceeding the water quantity of the aggregate.
In Fig. 3.13 is shown the evolution of four rain cells, 1 driver and 4 secondary daughters with initial parameters reported in Tab 3.2. The exchange is between the driver and the all secondary daughters in different moments with a checking for the exchange periodically effectuated every 100 s (set in the initial parameters).

Table 3.2: Initial parameters of the synthetic cells within the aggregate for the event Exchange

#Cell	R_p $[mm/h]$	$R_M(0)$ $[mm/h]$	ρ_0 $[km]$	k
Driver cell	150	48	6	288
Secondary cell 1	216	32	3	160
Secondary cell 2	211	32	3	160
Secondary cell 3	203	17	5	85

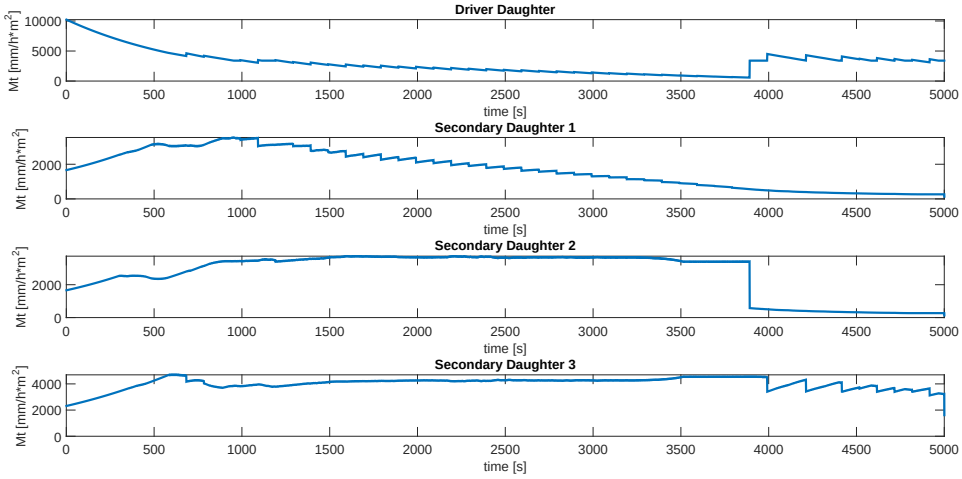

Figure 3.13: Example of evolution of the water quantity of the cells (1 initial driver daughter and 3 secondary daughter) inside the aggregate.

The abrupt interruptions on the curves are in correspondence of the exchanges but are only indicative because they refer on the nature of the cell, whether Driver or Secondary. For example in t=583 s the exchange is between Driver and Secondary 3 while in t=991 s the exchange is between Driver (the old Secondary 3) and Secondary 1. The application track all the exchanges and at the end of the simulation the histories of the parameters of each cell can be reconstructed. An example evolution of the peak rain rate R_M of the cells described in Tab. 3.2 is shown in the following figure.

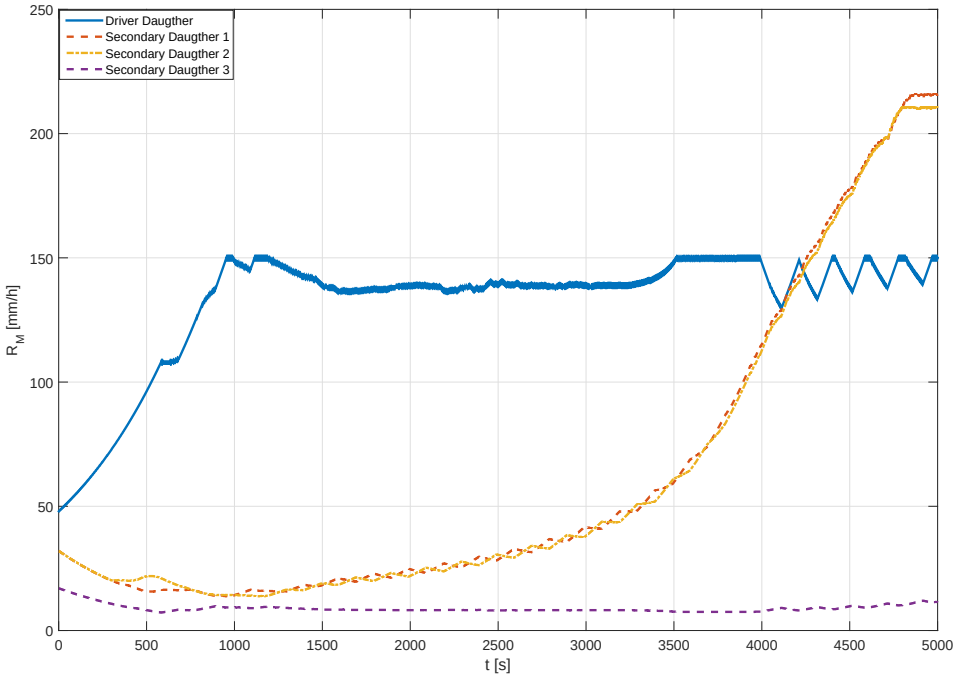

Figure 3.14: Example of evolution of the peak rain rate during the Exchange event.

In this last figure it is noticed that after t=4000 s, the evolution of R_M presents a fluctuation fairly strong. This is due to the exchange between the Driver Daughter and the Secondary Daughter 3. In this last part of the scene the two cells compete for the exchange and at each checking they change behavior.

3.4.4 Cells' elimination

The elimination phase starts when the R_M of a given cell reaches very low values, next to 5mm/h. Being 5mm/h the minimum value that the synthetic cell can have, the only way to reduce the area is to reduce the k parameter. Once this phase is started k will slowly decrease during the scene (for example k decrease linearly every second), in order to have a cell with a low rain rate peak and a small area (in nature this phenoma can be seen as a rain area that slowly dissolves). The secondary cell j-th with water quantity Q_j is effectively eliminated if the following condition occurs:

1. The water quantity Q_j at the time t is less than a threshold Q_{th} set initially, that depends on the initial value of Q_j (for example $Q_{th} = \epsilon Q_j$ with $\epsilon = 0.1$);

2. The elimination of a daughter must imply an overall error in the re-calculation of the new water quantity less than a threshold level that depends on what

is the error tolerated to the water quantity of the aggregate ($\epsilon' = 5\%$).

Being the error for the elimination in the second condition calculated on one cell, only one can be eliminated at the time t. For this reason if more cells satisfy these two conditions one of the competitors is chosen in a random manner and eliminated. This event is often associated to a scene where the water quantity of the aggregate is decreasing. In the figure is shown an example of elimination for a cluster of cells described in Tab. 3.3. The elimination happens when the water quantity of the cell is reduced at 10% with respect to its initial value. The cell eliminated is Secondary cell 1 at t=2526 s while, in this case, its competitor was the Secondary cell 3, that presentsan evolution towards higher value for the peak rain rate, as illustrated in Fig. 3.17.

Table 3.3: Initial parameters of the synthetic cells within the aggregate for the event Elimination

#Cell	R_p $[mm/h]$	$R_M(0)$ $[mm/h]$	ρ_0 $[km]$	k
Driver cell	150	30	6	180
Secondary cell 1	77	12	2	24
Secondary cell 2	63	25	2	50
Secondary cell 3	85	13	4	52
Secondary cell 4	79	17	2.5	42.5

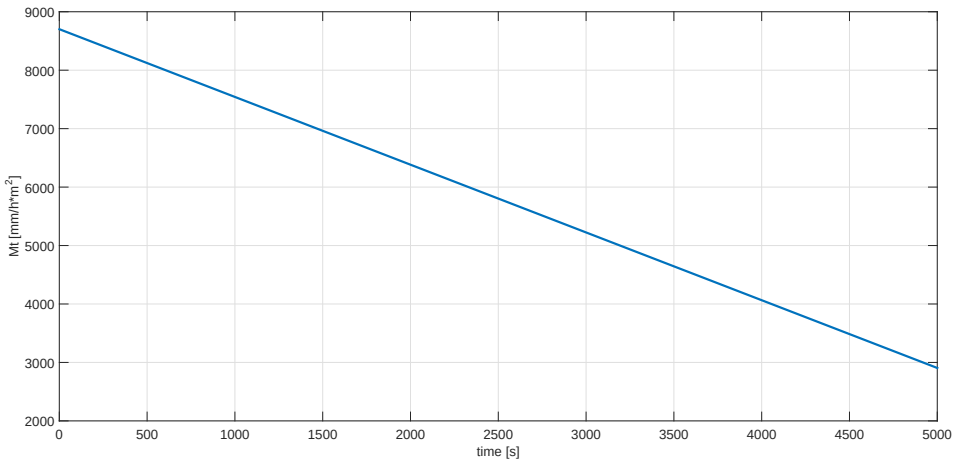

Figure 3.15: Evolution of the water quantity of the mother.

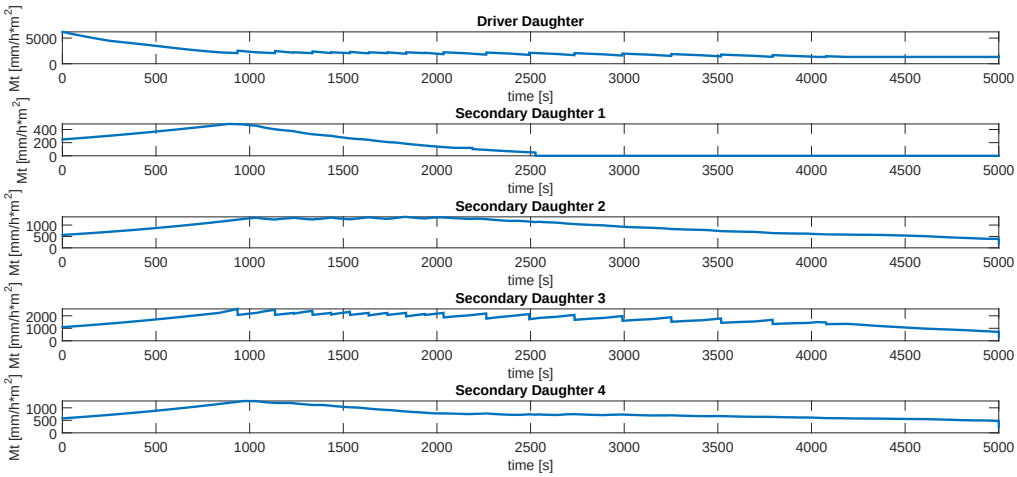

Figure 3.16: Example of evolution of the water quantity and handling of the Elimination event for Secondary Daughter 1.

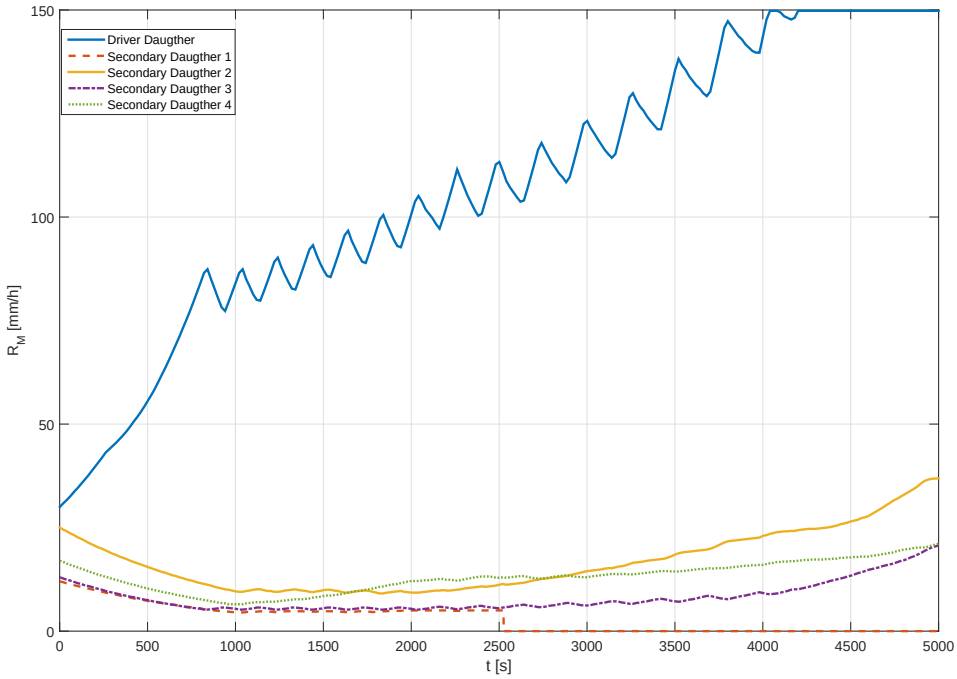

Figure 3.17: Evolution of the peak rain rate for each cell and handling of the elimination of Secondary Daughter 1.

The evolution of ρ_0 associated to R_M is shown in the next figure. It is noticed that ρ_0 at time t=326 s is not linked to R_M anymore k begins to decrease. Daughter cell 1 continues to evolve to maintain the water quantity of the aggregate until t=950 s. In that moment the water quantity could be maintained by the other daughters and Daughter cell 1 begins to decrease. At time t=2526 s the value of the water quantity is such that the cell can be effectively eliminated (the requirments for the elimination are satisfied).

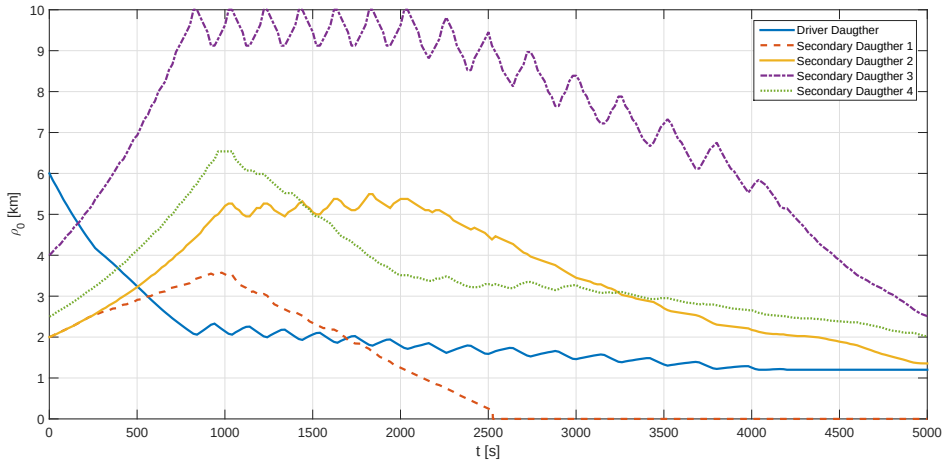

Figure 3.18: Evolution of the equivalent radius for each cell and handling of the elimination of Secondary Daughter 1. The reduction of k is $0.01/s$.

3.4.5 Calculus of the attenuation

The information recovered in the last section can be used to generate an aggregate that moves towards a given direction and that passes over a radio channel, utilizing the same application explained in Chapter 2. Given the initial position of each cells, the cells are positioned inside the matrix of the aggregate that is, in turned, positioned inside the matrix of the map. Fixed all the parameters just presented, as direction and velocity of the wind, transmitter and receiver positions, T_s, the simulation can start. An example of the result for the movement of the cell and the corresponding attenuation that affects the radio channel is illustrated in the next figures, respectively. The evolution of R_M and ρ_0 are related to the example of "Cell's elimination" presented in the previous section. The scene presents a possible real case: a base station, in the center of the map, communicates with a satellite (outside the map) with an elevation of 30.2°. The speed of the aggregate is 11.11 m/s, its height is of 3.35 km and the sampling of the attenuation is each 250 s.

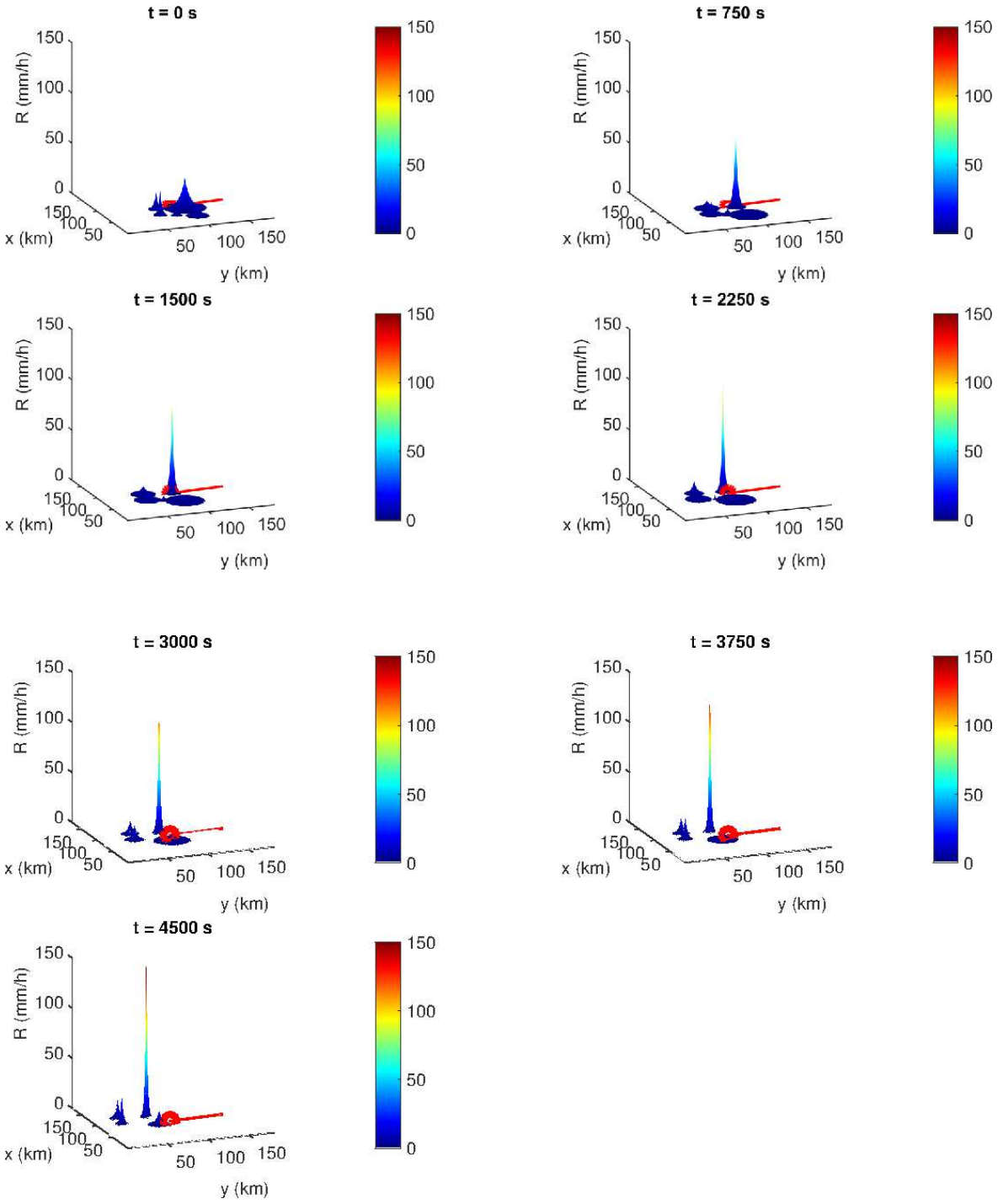

It is noticed that the small cell that initially is positioned approximately at the center of the map and that must be eliminated, for t=2250 s it is almost disappeared. The maximum on the attenuation will be during the transition of the Driver cell (the cell with the higher peak rain rate) over the base station (t=1250 s).

A further attenuation (after t=2500 s) will be given by the side of the last cell, Daughter cell 3, with a low peak rain rate and the widest radius.

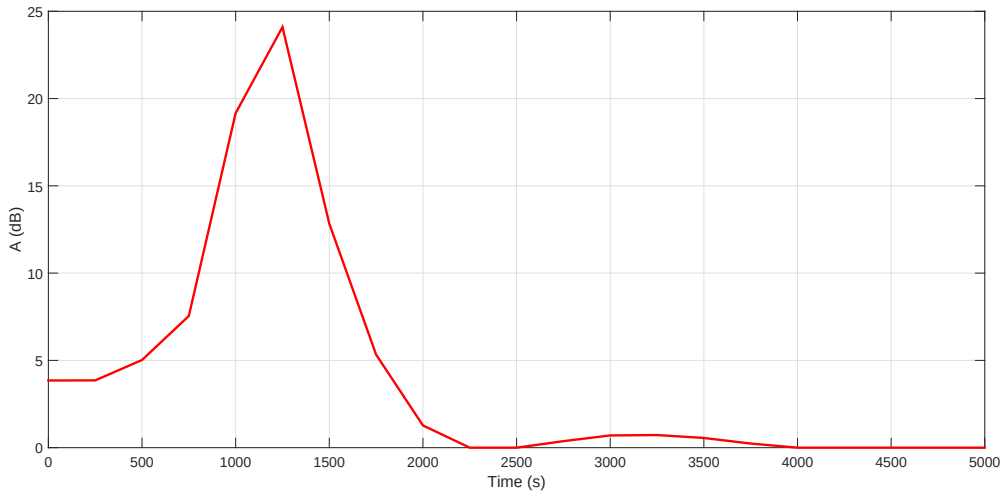

Figure 3.19: Attenuation experienced by the link, sampled every 250 s.

Conclusions and future works

In the entire project we referenced to the theoretical model EXCELL (that is turned out to be the best model to represent a synthetic cell) that describes the horizontal rain intensity profile by means of an exponential function (Chapter 1), mainly characterized by two parameters: the peak rain rate R_M, that define the rain intensity of the cell and the equivalent radius ρ_0, that define its spatial dimension.
On the basis of this model, the analysis focused on the development of two applications.

The first application (Chapter 2) described a scenario with a radio channel between two fixed stations affected by the attenuation due to a rain cell, modeled with the horizontal profile of the EXCELL, and with the capability to move inside the map and to change its horizontal profile during the scene. Once defined the environmental parameters utilized (map dimension and resolution, transmitter and receiver position, temporal resolution) and the physical parameters (velocity, direction, height of the rain cell), the temporal and spatial evolution of the horizontal profile are analyzed. In particular, for what concerns the temporal evolution, the values of the peak rain rate R_M are defined by the values red along a curve with a given maximum R_p following random directions. The change of R_M has been linked to ρ_0 ,and thus to the area of the cell, by means of a hyperbolic relation that states that to an increment of R_M corresponds a decrement ρ_0 and viceversa.
During its movement, the cell evolves and passes through the radio link introducing an attenuation that has been calculated. The results reports that an increase of the peak of the cell and in correspondence of the reduction of the area the attenuation tends to quickly decrease with respect to a static cell. On contrary, when the link is affected for a long time by the rain cell, due to the low displacement velocity of the rain cell in the map, the attenuation is higher for a cell that evolves toward high values of rain peak. For spatial communication it was noticed that the link is not strongly effected by rain because only a small portion of link passes through the rain cell. This is noticeable especially for the dynamic cell where the displacement velocity in addition with the reduction of the area leads to a fast leaving of the link from the rain cell.

In the second application, the concept of the profile temporal evolution has been extended to a set of more cells. The percentual evolution of the rainy coverage of the map was associated to the percentual evolution of the water quantity of the map, given by the sum of the water quantity of each rain cell inside the map in a given time, which are defined by different couple of parameters R_M and ρ_0 and clustered in a certain number of aggregate. For each aggregate has been calculated its water quantity inside the time window analyzed, such that the sum of their water quantity is equal to the water quantity of the map.
Each cell inside the aggregate, as observed in radar maps, presents two different behavior that has been implemented, on the basis of their nature. The former behavior is related to the evolution of the water quantity of the cell (daughter) defined as "driver", which has the greatest water quantity in the cluster of cells and that follows the evolution of the water quantity of the aggregate (mother). The latter behavior concerns the evolution of the other minor cells of the cluster that evolves in order to minimize the water quantity remaining, given by the difference between the water quantity of the aggregate and the water quantity of the "driver" cell.
Moreover, when some conditions are satisfied, the cells show different behaviors: they can be eliminated when their carrying amount of water becomes negligible compared to the amount of water of the entire aggregate; they can exchange among them, with the possibility of the promotion of a minor cell to "driver", when the aggregate amount of water of the driver becomes lower than the one of the secondary daughter.

The future works will focus on the extension of these applications, adding some aspects not considered in this work, that can be:

- the implementation of an elliptical cell instead of the circular one to better describe a real cell from the physical point of view;
- utilization of the data about the evolution of R_M and ρ_0 of each cell generated with the application discussed in Chapter 3 to create dynamic maps with the application of the Multiexcell model studied by Luini [11], that takes into account the spatial correlation characteristics of the rainfall related to the interdistance of the cells inside the aggregate and the interdistance between the aggregates in the map;
- The discrimination of the type of cell, whether uniform (with slow evolution and limited value of maximum peak rain rate) or convective, could lead to

a better choice of the maximum peak R_p. Furthermore, this classification could be an input to implement a system with a dynamic height of the cell or to implement the melting layer and the ice layer above. The implementation of the latter, that particularly affects stratiform rainfall, could be useful to take into account, beyond the attenuation, also the depolarization of the signal.

Bibliography

[1] A. Adhikari, S. Das, A. Bhattacharya, and A. Maitra, "Improving rain attenuation estimation: Modelling of effective path length using ku-band measurements at a tropical location," *Progress In Electromagnetics Research B*, vol. 34, pp. 173–186, 2011.

[2] L. J. Ippolito, "Radio propagation for space communications systems," *Proceedings of the IEEE*, vol. 69, no. 6, pp. 697–727, 1981.

[3] L. Luini and C. Capsoni, "Multiexcell: a new rainfall model for the analysis of the millimetre wave propagation through the atmosphere," in *Antennas and Propagation, 2009. EuCAP 2009. 3rd European Conference on*, pp. 1946–1950, IEEE, 2009.

[4] C. Capsoni and L. Luini, "Analysis of the spatial and temporal properties of rain cells for rainfall modeling purposes," *Ital. J. Remote Sens*, vol. 41, no. 3, pp. 51–62, 2009.

[5] C. Capsoni, F. Fedi, C. Magistroni, A. Paraboni, and A. Pawlina, "Data and theory for a new model of the horizontal structure of rain cells for propagation applications," *Radio Science*, vol. 22, no. 3, pp. 395–404, 1987.

[6] L. Féral, H. Sauvageot, L. Castanet, and J. Lemorton, "Hycell-a new hybrid model of the rain horizontal distribution for propagation studies: 1. modeling of the rain cell," *Radio Science*, vol. 38, no. 3, 2003.

[7] H. Lam, L. Luini, J. Din, C. Capsoni, and A. Panagopoulos, "Application of the sc excell model for rain attenuation prediction in tropical and equatorial regions," in *Applied Electromagnetics (APACE), 2010 IEEE Asia-Pacific Conference on*, pp. 1–6, IEEE, 2010.

[8] L. Luini, N. Jeannin, C. Capsoni, A. Paraboni, C. Riva, L. Castanet, and J. Lemorton, "Weather radar data for site diversity predictions and evaluation of the impact of rain field advection," *International Journal of Satellite Communications and Networking*, vol. 29, no. 1, pp. 79–96, 2011.

[9] "Specific attenuation model for rain for use in prediction methods," International Telecommunication Union, 2005. Recommendation ITU-R P.831-1.

[10] "Rain height model for prediction methods," International Telecommunication Union, 2013. Recommendation ITU-R P.839-4.

[11] L. Luini, C. Capsoni, M. D'Amico, and P. Colaneri, *MultiEXCELL: a large-scale rain field model for propagation applications and its experimental identification (Alphasat)*. PhD thesis, Doctoral Dissertation, 2009.

[12] S. A. Stoica, "Analysis of the temporal evolution of rain cells for propagation applications," 2009. Master thesis.